BMC Plant Biology

RESEARCH

Open Access

Glutathione S-transferase in mediating adaptive responses of oats (*Avena sativa*) to osmotic and cadmium stress: genome-wide analysis

Chenbiao Xu[1,2,3†], Lyu Jiang[1,2†], Aixue Li[1,2†], Jie Meng[1,2,7], Ping Yun[4], Jianfang Li[3], Changbin Liu[8], Yang Chen[1,2], Han Zhang[1,2], Hassan Ahmed Ibraheem Ahmed[6], Quan Gao[1,2], Lana Shabala[4,5], Sergey Shabala[4,5*], Bin Luo[1,2*] and Peichen Hou[1,2*]

Abstract

Background Glutathione S-transferases (GSTs) are essential multifunctional enzymes. In the face of abiotic stresses such as drought and heavy metal exposure, plants utilize GSTs for detoxification and antioxidant defense, as these enzymes facilitate the conjugation of glutathione (GSH) with toxic compounds. Specific details of this process, however, remain unknown.

Results This study identified 118 *Avena sativa GST* (*AsGST*) genes within the *A. sativa* genome and classified them into five subfamilies: Tau, Phi, Zeta, Lambda, and EF1Bγ. Phylogenetic analysis revealed that *AsGSTs* exhibit significant similarity to corresponding *GST* categories in *Arabidopsis thaliana* and *Oryza sativa*, indicating a possible common ancestor. Gene structure and conserved motif analysis demonstrated that *AsGST* genes within the same subfamily shares similarities in the number and positioning of exons and introns, as well as in motif composition, suggesting that these genes may perform analogous biological functions in *A. sativa*. The promoter regions of the identified genes are enriched with various cis-acting elements that play roles in plant growth and development, stress response, and hormone signaling. Transcriptomic analysis and real-time quantitative PCR (RT-qPCR) validation indicated that the expression of four *AsGST* genes (*AsGSTU12*, *AsGSTU13*, *AsGSTU14*, and *AsGSTU15*) was significantly up-regulated in the roots of *A. sativa* under both PEG-induced drought stress and $CdCl_2$-induced cadmium stress. These genes likely regulate reactive oxygen species (ROS) levels by catalyzing their scavenging through glutathione (GSH) substrates, and may also participate in ABA signaling and the maintenance of osmotic homeostasis. Under cadmium stress, these genes may mitigate cadmium toxicity by enhancing the chelation and sequestration of cadmium via GSH or through its compartmentalization, as evident from the subcellular localization studies.

†Chenbiao Xu, Lyu Jiang and Aixue Li contributed equally to this work.

*Correspondence:
Sergey Shabala
sergey.shabala@uwa.edu.au
Bin Luo
luob@nercita.org.cn
Peichen Hou
houpc@nercita.org.cn
Full list of author information is available at the end of the article

Conclusion This study systematically described the *GST* gene family in *A. sativa*, characterized its expression patterns and potential functions in response to drought and cadmium stress, and confirmed the essential role of the *AsGST* gene family in mediating stress responses. The findings enhance our understanding of the mechanisms underlying stress tolerance and offer valuable genetic resources for breeding stress-tolerant *A. sativa*. The work also provides a theoretical framework and identifies gene targets for the development of stress-resistant *A. sativa* varieties.

Keywords *GST* genes, Phylogenetic analysis, Osmotic stress, Cadmium stress, ROS

Background

Glutathione S-transferases (GSTs) represent a diverse group of multifunctional enzymes prevalent in plants, where they are essential for growth, development, and responses to environmental stresses [1]. These enzymes facilitate various biological processes, including detoxification metabolism, antioxidant defense, and signaling, by catalyzing the conjugation of glutathione (GSH) to electrophilic compounds [2–4]. A typical GST comprises two distinct binding sites, which are located at the N- and C- terminus, to bind GST (GST-N) and neighboring substrate (GST-C), respectively [5, 6]. Based on similarities in the sequence and structural as well as their functional roles, plant *GST* genes are categorized into 14 subfamilies, including Phi (F-type), Tau (U-type), Lambda (L-type), Theta (T-type), Zeta (Z-type), dehydroascorbate reductase (DHAR), γ-subunit of the eukaryotic translation elongation factor 1B (EF1Bγ), tetrachlorohydroquinone dehalogenase (TCHQD), metaxin, Ure2p, Hemerythrin (H), Iota (I), microsomal prostaglandin E-synthase type 2 (mPGES- 2), and glutathionyl-hydroquinone reductase (GHR) [7]. Notably, the Tau, Phi, Lambda, and TCHQD subfamilies are exclusive to plants and play pivotal roles in xenobiotic metabolism by binding a broad spectrum of harmful exogenous compounds, such as insecticides and herbicides, thus safeguarding plants from toxic effects [8].

The multifunctionality of GSTs is evidenced by their involvement in regulation plant ROS signalling, redox balance, and hormone biosynthesis [9]. GSTs are intricately linked to biotic and abiotic stresses [10] and are vital for plant growth, development, and enhanced stress tolerance, playing a crucial role in the antioxidant defense mechanism [11]. The expression and activity of GSTs significantly bolster plant adaptation to various stress conditions, including low temperatures, high salinity, drought, and heavy metal exposure [12]. For instance, under salt stress, *GSTs* in *Gossypium hirsutum* exhibit tissue-specific expression patterns [13], while the *SlGSTU43* gene in *Solanum lycopersicum* aids in scavenging ROS and promoting lignin biosynthesis, both of which enhance salt stress tolerance [14]. In poplar, *PtGSTF1* improves ion homeostasis and ROS scavenging under salinity stress [15] while in *Juglans regia* the *JrGSTTau1* gene enhances cold tolerance [16]. Similarly, the *IbGST4* and *IbGST2* genes mitigate low-temperature-induced ROS accumulation and associated damage [17].

Also significant is the role of *GST* in responding to drought and heavy metal stress. For example, *CsGSTU8* in *Camellia sinensis* positively regulates drought stress, modulated by the transcription factor (TF) *CsWRKY48* [18]. In *Pisum sativum* GST activity was elevated in plants subjected to cadmium stress [19]. Ectopic expression of *OsGSTU4* and *OsGSTU30* from rice has been shown to enhance the tolerance of transgenic *Arabidopsis thaliana* to salinity, oxidative stress, drought, and heavy metal stress [20, 21]. These findings highlight the growing importance of *GST* in addressing drought and heavy metal stress, suggesting potential strategies for the development of resilient crops capable of thriving in challenging environmental conditions. However, given the plethora of GST isoforms, it remains to be answered what are their specific roles, and which of them may be a suitable target for improving abiotic stress tolerance in crops.

Avena sativa (*A. sativa*) is a heterozygous hexaploid crop (AACCDD, 2n = 6x = 42) belonging to the genus Avena in the family *Poaceae*. It is extensively cultivated in 42 countries and territories worldwide due to its economic and nutritional significance [22], ranking as the sixth highest in global production [23]. *A. sativa* is recognized for its low carbon footprint and a wealth of health benefits, characterized by high concentrations of soluble fiber, β-glucan, lipids, proteins, and antioxidants [24]. Furthermore, *A. sativa* serves as a nutritious forage grass [25], demonstrates adaptability to diverse soil conditions, and shows significant drought tolerance [26], as well as considerable resistance to heavy metals [27]. Investigating the molecular mechanisms underlying drought tolerance and heavy metal resistance in *A. sativa* is essential for elucidating its stress tolerance strategies. The availability of genomic information for *A. sativa* enables in-depth exploration of the molecular mechanisms governing growth, development, and stress regulation at the genomic level [28, 29]. This research provides a foundation for a comprehensive study of the *GST* gene family and holds significant

potential for guiding molecular breeding efforts aimed at enhancing resistance traits in *A. sativa*.

In this study, we identified the *GST* gene family members in *A. sativa* through bioinformatics analysis, focusing on chromosomal localization, phylogenetic relationships, conserved structural domains, gene structures, and gene duplication events. Additionally, we examined the expression profiles of four *AsGST* genes in roots subjected to PEG-induced drought stress and $CdCl_2$-induced cadmium stress at various time points, utilizing transcriptomic data and real-time quantitative PCR (RT-qPCR) technology. The results from both datasets exhibited a high degree of consistency, providing a robust basis for further validation of the functions of these four genes in response to drought and cadmium stress.

Results

Identification of GSTs in *A. sativa*

In this study, the protein sequences of 53 AtGST (Table S1) and 77 OsGST (Table S2) were utilized for the preliminary screening of the *A. sativa* genome via BLASTP and HMMER tools. Following further validation using CD-HIT software and the NCBI-CDD and SMART databases, a total of 118 non-redundant *AsGST* full-length genes, each containing complete GST_C and GST_N structural domains, were identified. The physicochemical properties of these AsGST proteins were assessed (Table S4), revealing protein lengths ranging from 178 amino acids (AsGSTF18) to 467 amino acids (AsEF1G4), with an average length of 248 amino acids. The molecular weights (MWs) of the AsGST proteins varied from 20.43 to 52.76 kDa, while isoelectric point (PI) values spanned from 4.79 to 7.82. Notably, five proteins (AsGSTU24, AsGSTF40, AsGSTF10, AsGSTF43, and AsGSTF3) exhibited PI values greater than 7, indicating a more basic nature compared to the other 173 proteins. Regarding subcellular localization, the majority of AsGST proteins were predicted to reside primarily in the cytoplasm and chloroplasts, with additional localization in the nucleus, extracellular matrix, peroxisomes, mitochondria, and vesicles. Furthermore, most AsGST proteins were classified as stable (instability index < 40); however, 46 proteins were identified as unstable, suggesting that while AsGST proteins are generally stable, some are prone to degradation. Additionally, only 21 proteins exhibited a hydrophobicity index greater than 0, indicating that most AsGST proteins are hydrophilic.

Phylogenetic analysis of GSTs in *A. sativa*

To investigate the evolutionary relationships among the GST proteins of AtGST, OsGST, and AsGST, a phylogenetic tree was constructed (Fig. 1). The *AsGST* gene family was classified into five distinct subfamilies based on the subfamily classifications of *A. thaliana* and *Oryza sativa*. Among these, the Phi subfamily contained the largest number of *AtGST* genes (59), followed by the Tau subfamily (50), while the Zeta and EF1Bγ subfamilies each had one member, as did the Lambda subfamily. Although subfamilies Theta, DHAR, and TCHQD are present in both *A. thaliana* and *O. sativa*, corresponding members were absent in *A. sativa*. Furthermore, no distinct clusters were identified for the Zeta and Lambda subfamilies, underscoring the considerable homology among AsGST members within each subfamily.

Analysis of the gene structure and motifs in *A. sativa*

To further investigate the interrelationships among the *AsGST* family genes, we predicted the conserved motifs of the AsGST proteins using the MEME suite, identifying a total of ten conserved motifs. Concurrently, the conserved structural domains of AsGST proteins were predicted with the NCBI-CDD tool. The distribution of the structural features, conserved motifs, and conserved structural domains of the *AsGST* genes is illustrated in Fig. 2. Results revealed that members of the same subfamily exhibit high similarity in conserved motif distribution, with motif 1 being the most conserved and, presenting across all members. With the exceptions of AsGSTL1 and AsGSTZ1, no significant differences in the number of conserved motifs were observed among the remaining GST sequences. Notably, specific motifs were exclusive to certain subfamilies; for instance, motif 7 was restricted to the Phi subfamily, while motifs 8 and 9 were unique to the Tau subfamily (Fig. 2B). These findings imply that members within the same subfamily may share functional similarities, whereas different subfamilies might display functional differentiation due to the specificity of their conserved motifs. A similar pattern emerged from the analysis of conserved structural domains, where GST sequences from the same subfamily possess highly similar domains, while unique structural domains were identified across different subfamilies. For example, only the EF1Bγ class *GST* genes contained the EF1G superfamily conserved structural domain (Fig. 2C), reinforcing the notion of functional similarity within subfamilies and potential functional differentiation between them. Additionally, we examined the coding sequences (CDS) and non-coding regions (UTRs) of the *AsGST* gene family (Fig. 2D). The number of exons varied from 1 to 11, with AsGSTL1 and AsGSTZ1 exhibiting the highest exon count of 11, while AsGSTU6, AsGSTU7, AsGSTU16, AsGSTU19, AsGSTU22, AsGSTU29, AsGSTU47, and AsGSTU49 each contained only one exon. Regarding introns, apart from

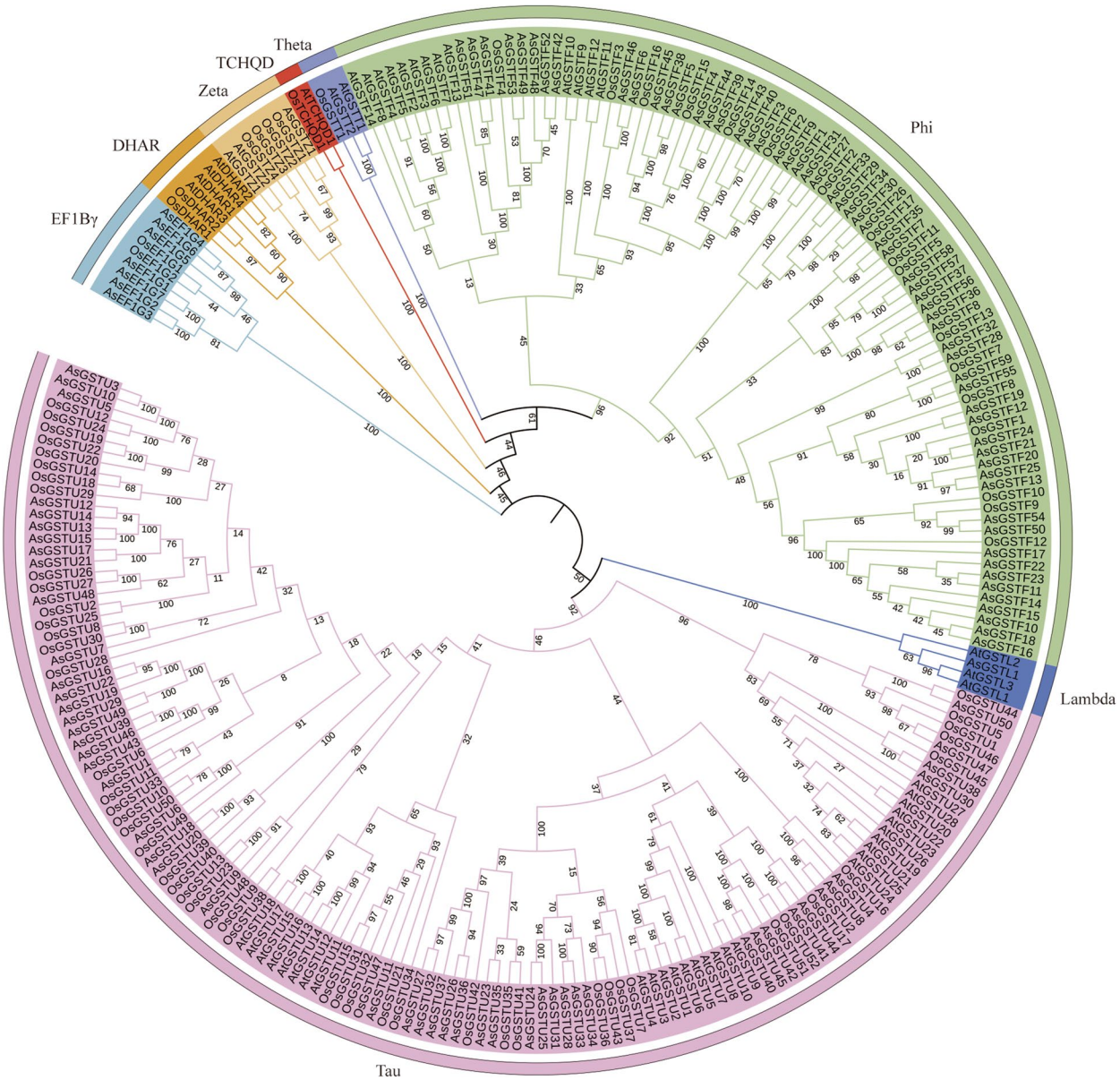

Fig. 1 Phylogenetic tree of GSTs from *A. sativa* (*AsGST*), *A. thaliana* (*AtGST*), and *O. sativa* (*OsGST*). These can be divided into eight subgroups (Tau, Lambda, Phi, Theta, TCHQD, Zeta, DHAR, and EF1Bγ); the different subgroups are distinguished by color

AsGSTL1 and AsGSTZ1, which contained 8 introns, eight genes lacked introns entirely, and the remaining *AsGST* family members exhibited intron counts ranging from 1 to 7. Collectively, these results suggest notable differences in gene structure, conserved motifs, and structural domains among *AsGST* genes across different subfamilies, potentially contributing to variations in their physiological functions. Nonetheless, the overall genetic structure of the *AsGST* gene family appears conserved, particularly among members of the same subfamily, which may indicate shared functional roles.

Promoter cis-acting element analyses in *A. sativa*

Using the PlantCARE online platform, we analyzed the cis-responsive elements present in the promoter regions of 118 *AsGST* gene sequences, extending approximately 2000 bp upstream of the transcriptional start site. The identified cis-acting elements in the *AsGST* gene promoters are depicted in Fig. 3. In total, 25 distinct

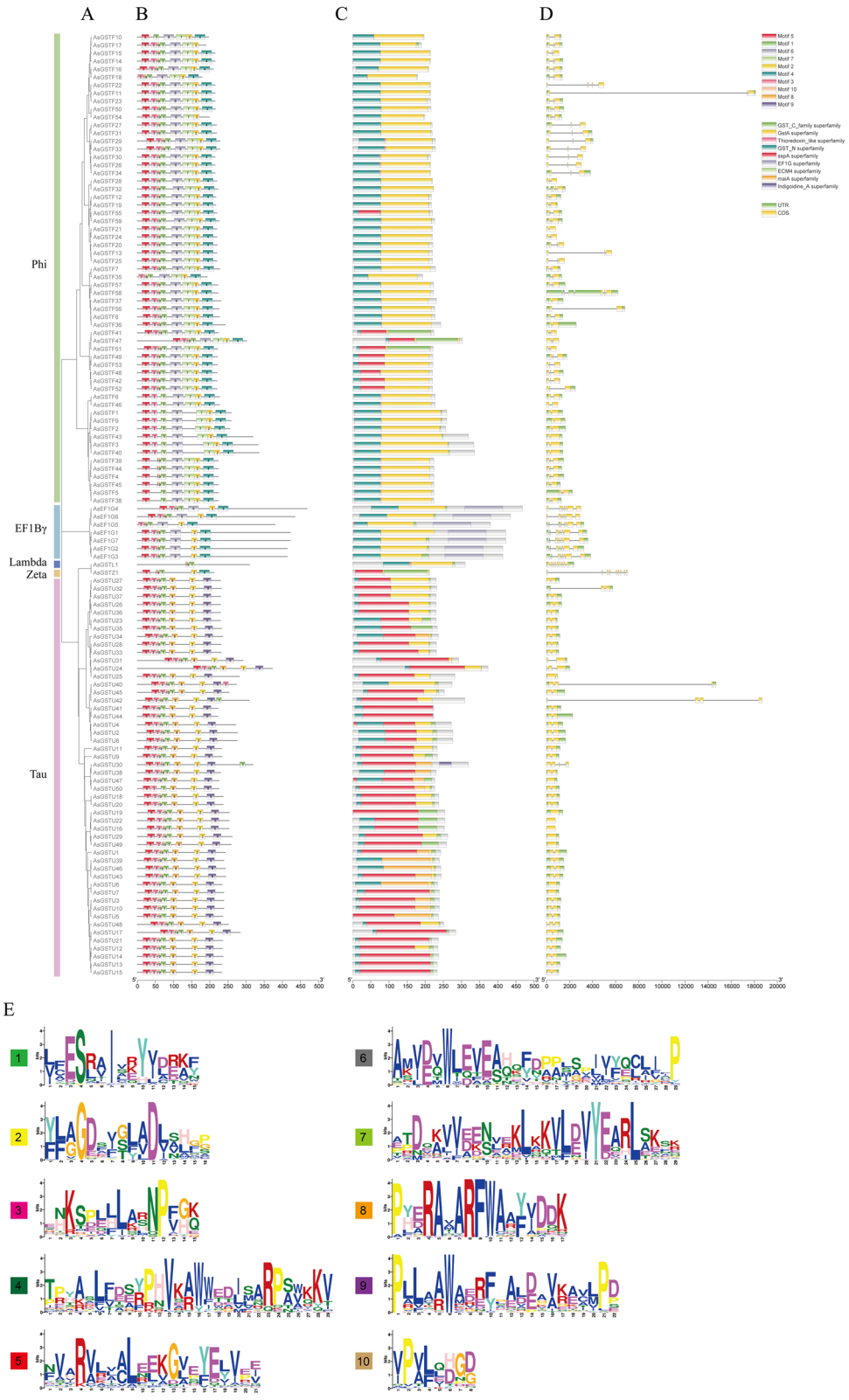

Fig. 2 Phylogenetic analysis, conserved motifs, conserved domains, and exon/intron structure of *AsGSTs*. **A** A phylogenetic tree constructed based on the full-length sequences of AsGST proteins using the maximum likelihood method, with 1000 bootstrap replicates. **B** Conserved motifs 1–10 are represented by boxes of different colors. **C** Conserved domains are represented by boxes of different colors. **D** Non-coding regions are indicated by yellow boxes; exons are indicated by green boxes; introns are indicated by black lines. **E** Consensus sequence of each motif

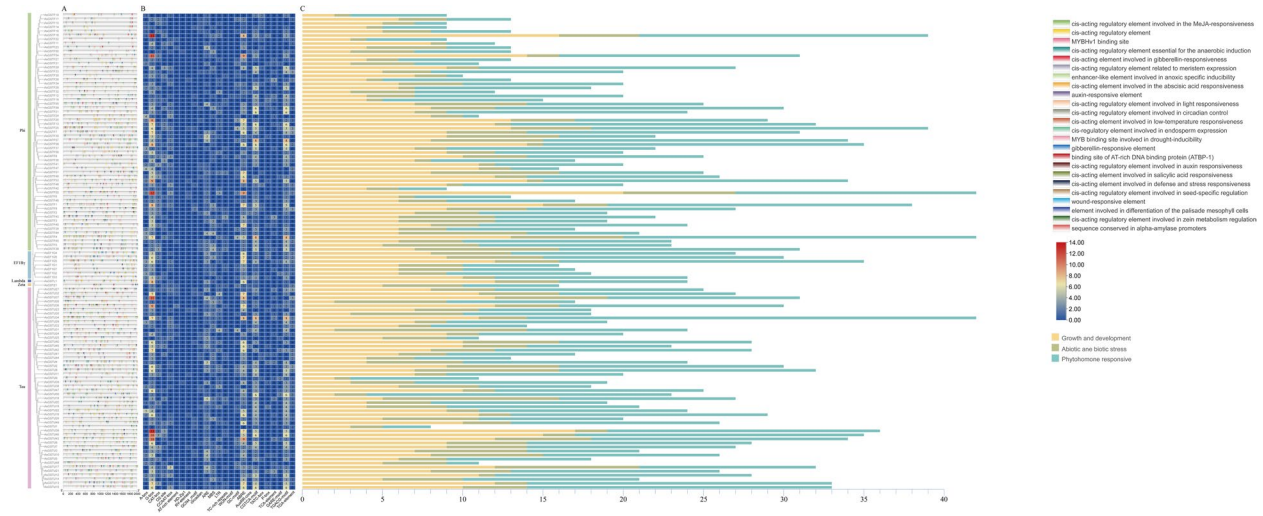

Fig. 3 Analysis of cis-acting elements in the promoter region of *AsGST*. **A** Visualization of cis-regulatory elements in the promoters of *AsGST* gene family members. **B** A heatmap displays the diversity of promoter elements in *AsGST* genes, with different colors and numbers representing different frequencies. **C** A histogram shows the cumulative counts of cis-acting elements in each category, represented by different colors

cis-responsive elements were recognized within the *AsGST* gene family, classified into three functional categories: plant growth and development, abiotic and biotic stress responses, and phytohormone responses (Fig. 3B).

Within the plant growth and development category, G-box elements were the most abundant, constituting 51.03% of all identified elements and 17.49% of the total elements, primarily regulating transcription initiation frequency. Additionally, we identified A-box, CAT-box, O_2-site, and circadian elements linked to photorespiration and metabolic regulation; CCAAT-box and AT-rich elements associated with transcriptional regulation; RY-element and GCN4_motif elements related to seed development; as well as the HD-ZIP1 element pertinent to flower and fruit development. The diversity and complexity of these elements underscore the significant role of *AsGST* genes in plant growth and development. The second category encompasses elements related to abiotic and biotic stress responses, including ARE and GC-motif elements associated with anaerobic conditions, MBS elements tied to drought stress, LTR elements linked to low-temperature response, TC-rich repeats involved in plant defense mechanisms, and WUN-motif elements relevant to wound response. Notably, ARE elements were the most prevalent in this category, representing 36.50% of abiotic and biotic stress response elements and 6.33% of all elements, indicating the potential significance of *AsGST* genes in mediating plant responses to environmental stresses. The third category involves hormone-responsive elements, which include those for abscisic acid (ABRE elements), growth hormones (AuxRR-core and TGA-element elements), salicylic acid (CGTCA-motif and TCA-element elements), gibberellin (TATC-box, P-box, and GARE-motif elements), and jasmonic acid (TGACG-motif element). These hormonal elements play crucial roles in plant development and stress responses. Among these, ABRE elements were the most, accounting for 29.95% of hormone-responsive elements and 14.49% of all elements (Fig. 3C). Overall, the analysis of promoter regions highlights the multifunctionality of *AsGST* genes in plant growth and development, stress responses, and hormone signaling, operating through interactions with various cis-responsive elements.

Chromosome distribution and gene replication in *A. sativa*

Based on the annotation file of *A. sativa*, we mapped the chromosomal localization of *AsGST* genes (Fig. 4). The analysis revealed a heterogeneous distribution of the 118 *AsGST* genes across the 21 chromosomes, with a notable prevalence of genes located in both proximal and distal regions. Specifically, chromosome 4D (chr4D) harbored the greatest number of *AsGST* genes, with a total of 16, followed by chr1D with 12 genes and chr4 A with 11 genes. Conversely, chr6 C contained the fewest *AsGST* genes, with only 1 gene identified. This distribution pattern may be closely linked to the functional roles of *AsGST* genes. Gene duplication, through tandem or segmental mechanisms, is a common evolutionary phenomenon in plants that significantly contributes to genome amplification and diversification (Fig S1). To further investigate the evolutionary dynamics of the *AsGST* gene family, we analyzed the gene duplication events using the MCScanx tool (Fig. 5A). Our results indicated that 30 *AsGST* genes were involved in tandem duplication

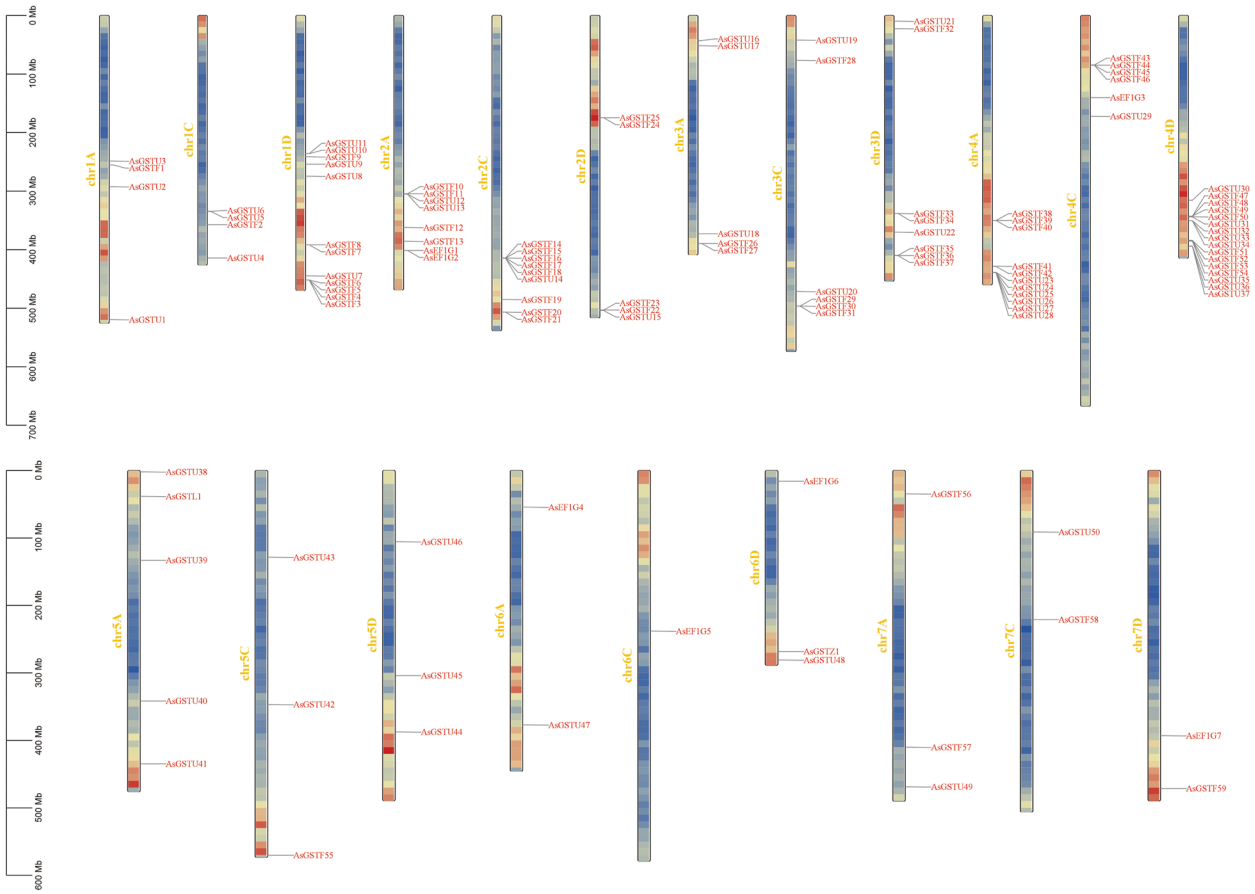

Fig. 4 Distribution of *AsGST* on *Avena sativa* chromosomes. The chromosomal positions of each *AsGST* gene were mapped onto the *A. sativa* genome

events, organized into 14 distinct clusters. Among these tandem duplications, 9 pairs were classified within the Phi subfamily, 4 pairs in the Tau subfamily, and 1 pair in the EF1Bγ subfamily. Additionally, we identified 109 segmental duplication pairs comprising 74 genes, suggesting that these duplication events may have played a crucial role in the expansion and functional diversification of the gene family. To assess the selective pressures acting on the duplicated genes, we calculated the ka/ks ratios. The results indicated that all gene pairs exhibited ka/ks values less than 1, ranging from 0.03 to 0.78, implying that purifying selection has been a significant force in the evolution of these *AsGST* gene pairs (Table S5).

To further elucidate the phylogenetic mechanisms and conserved genomic structure of the *AsGST* gene, we examined the covariance between *A. sativa* with *A. thaliana*, *O. sativa*, and *Triticum aestivum* (Fig. 5B). Our analysis revealed a single pair of segmental duplications in the *GST* gene between *A. sativa* and *A. thaliana*, whereas there were 36 and 63 pairs of segmental duplications identified between *O. sativa* and *T. aestivum*, respectively. This disparity highlights a closer genomic relationship between *A. sativa* and both *O. sativa* and *T. aestivum*, particularly in the expansion and conservation of the *GST* gene family. These findings suggest shared molecular mechanisms that facilitate adaptation to environmental stresses and evolutionary processes among these species. The observed conservatism may stem from the common ancestry and similar genomic evolutionary histories shared by *A. sativa*, *O. sativa*, and *T. aestivum*. In contrast, *A. thaliana*, as a dicotyledonous crucifer, exhibits a relatively distant genetic relationship with *A. sativa*.

Expression of AsGST under osmotic/drought stress conditions in *A. sativa*

In our investigation into the involvement of *AsGST* genes in the drought stress response of *A. sativa*, we analyzed changes in the expression of 118 *AsGST* genes in the root system of *A. sativa* using transcriptomic data sourced from the NCBI database (https://www.ncbi.nlm.nih.gov/bioproject/PRJNA1056521/). Our analysis

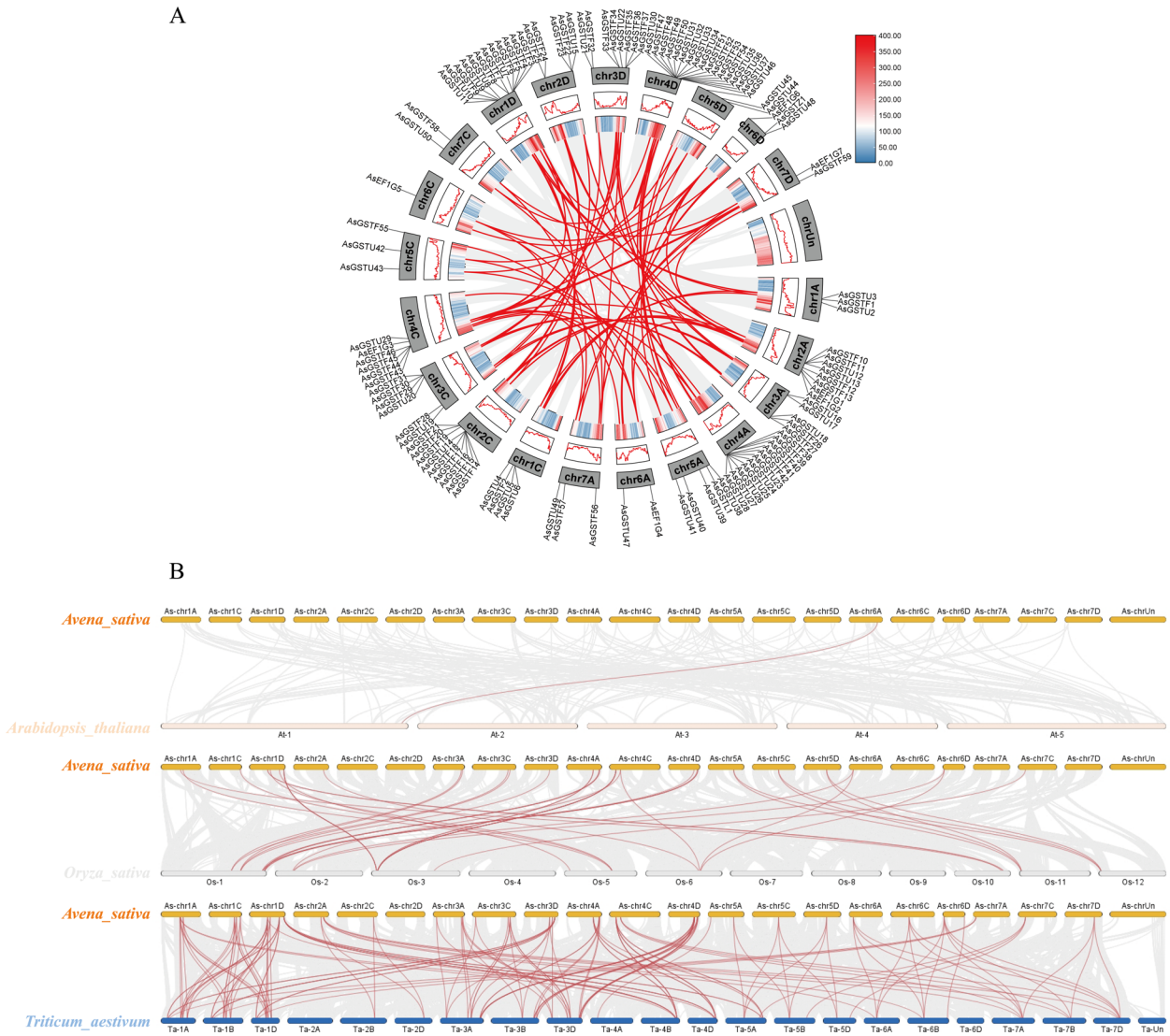

Fig. 5 Collinearity analysis of *AsGST*. **A** Intraspecific collinearity analysis of *AsGST* (paralogous gene pairs are highlighted by red lines. Gene density distribution on chromosomes is represented by a heatmap and dashed lines.) **B** Collinearity analysis of *AsGST* in *Arabidopsis thaliana*, *Oryza sativa*, *Triticum aestivum*, and *Avena sativa* (collinear *GST* gene pairs are indicated by red lines, while collinear regions between genomes are indicated by gray shading)

revealed a lack of detectable expression in 13 of these genes across all treatment times, while 83 genes showed no significant variation in expression (Fig. 6A, Table S6). Notably, 22 genes exhibited significant alterations in expression, among them 15 from the Tau subfamily (*AsGSTU6* to *AsGSTU18*, *AsGSTU21*, *AsGSTU37*, *AsGSTU43*, *AsGSTU45*) and seven from the Phi subfamily (*AsGSTF12*, *AsGSTF21*, *AsGSTF24*, *AsGSTF33*, *AsGSTF36*, *AsGSTF57*, *AsGSTF58*). In particular, *AsGSTU37* showed marked down-regulation for drought (PEG) treatment (osmotic stress mimicking drought conditions in the soil), especially at the initial stages (6 h and 12 h) where expression levels dropped by approximately threefold and sixfold. The other 21 genes showed significantly up-regulated expression (Table S6). Following these findings, we selected four genes showing similar expression patterns for confirmation via real-time quantitative PCR (RT-qPCR) from samples exposed to PEG treatment. To bolster the reliability of our experiment, in addition to validating the root transcriptome data, we quantified the gene expression levels in the leaves of *A. sativa*, and extended the treatment duration to 48 h. The RT-qPCR results (Fig. 7B) revealed dynamic, generally increasing expression patterns in roots for *AsGSTU12*,

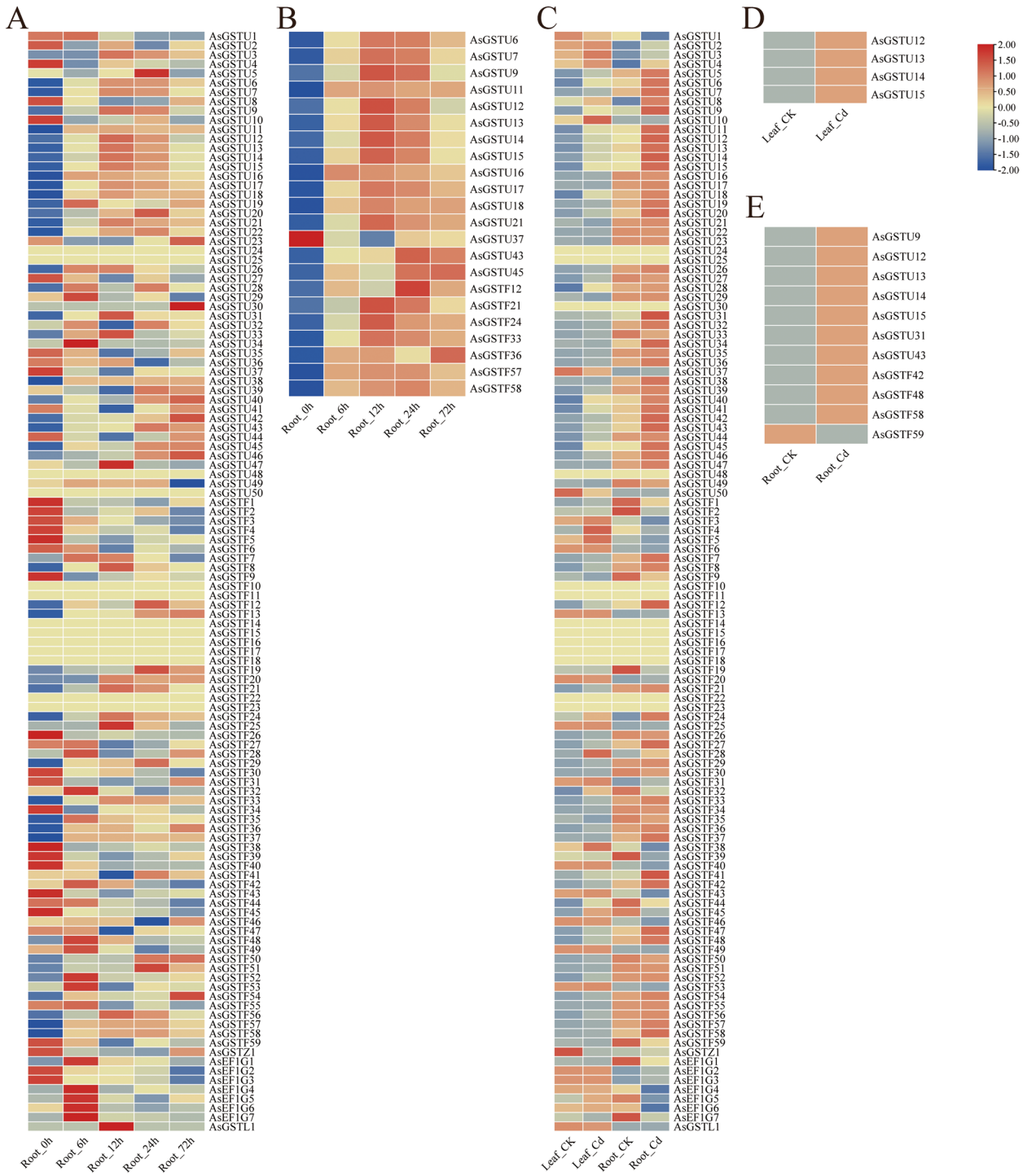

Fig. 6 Transcript abundance map of *AsGST*. **A** A heatmap shows the expression profiles of *AsGST* genes in roots under drought stress; **B** A heatmap shows the expression profiles of 22 differentially expressed genes in roots under drought stress; **C** A heatmap shows the expression profiles of *AsGST* genes in leaves and roots under cadmium stress; **D** A heatmap shows the expression profiles of 4 differentially expressed genes in leaves under cadmium stress; **E** A heatmap shows the expression profiles of 11 differentially expressed genes in roots under cadmium stress

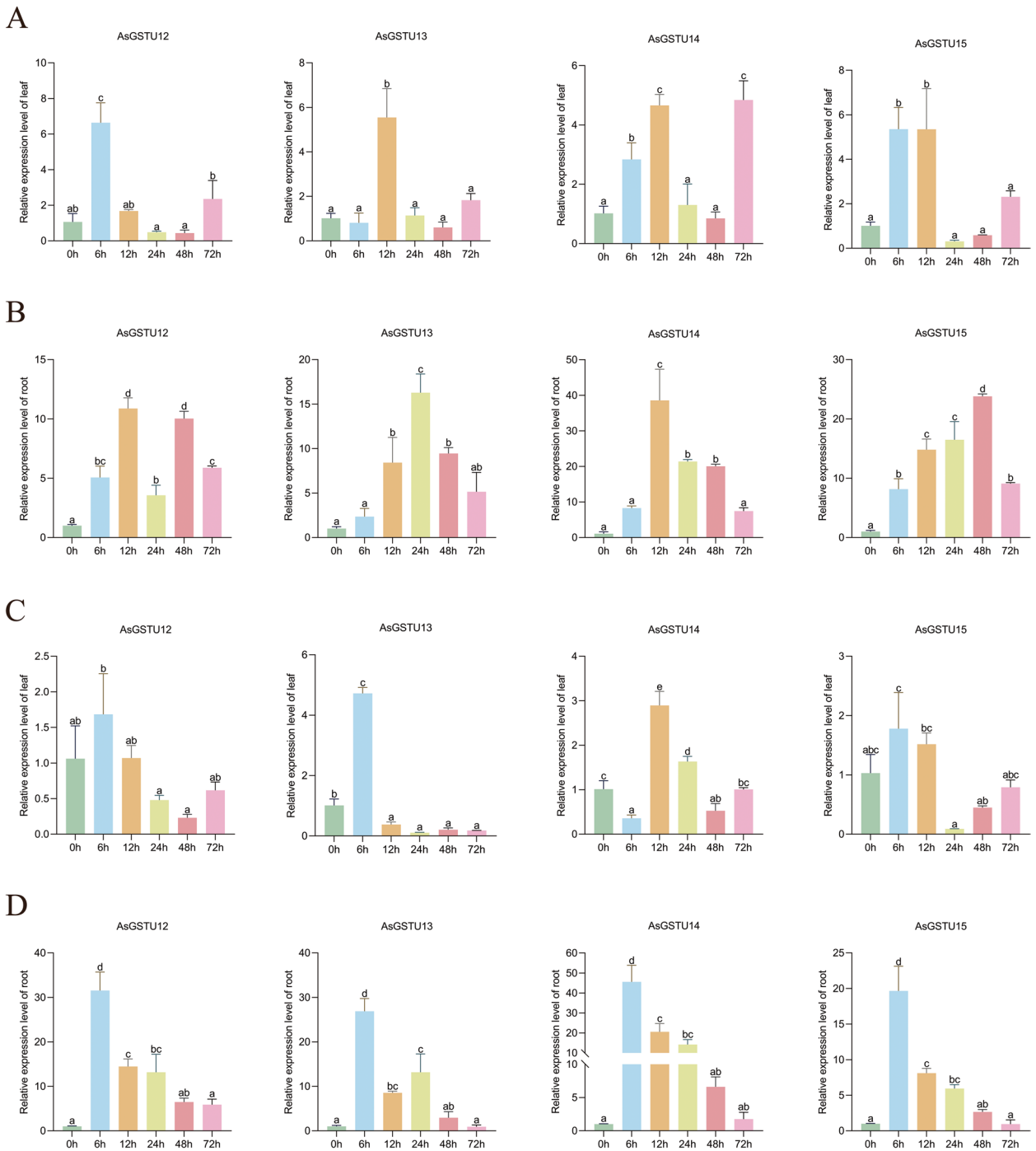

Fig. 7 RT-qPCR analysis of four differentially expressed genes. **A** Relative expression levels of four genes in leaves after PEG treatment; **B** Relative expression levels of four genes in roots after PEG treatment; **(C)** Relative expression levels of four genes in leaves after $CdCl_2$ treatment; **D** Relative expression levels of four genes in roots after $CdCl_2$ treatment. The Y-axis and X-axis represent the six time points of treatment and relative expression levels, respectively. The relative expression levels of the genes at 0 h were set to 1 and calculated using a normalization method. The mean ± standard deviation (SD) was obtained from three biological replicates and three technical replicates. Error bars indicate the standard deviation. Different letters indicate significant differences at $P < 0.05$ level, while the same letters indicate no significant differences

peaking at 12 h and 48 h with about tenfold up-regulation, though at 24 h, the expression fell but remained approximately threefold above control levels. Similarly, *AsGSTU13*, *AsGSTU14*, and *AsGSTU15* showed trends of initial increase followed by a decrease, with *AsGSTU13* expression levels rising from around twofold up-regulation at 6 h to 16-fold at 12 h, before gradually falling to fivefold at 72 h (Fig. 7B). Conversely, in *A. sativa* leaves, the expression patterns of these four genes differed (Fig. 7A). Significant up-regulation was observed in the early stages of drought treatment (6 h or 12 h), but expression levels significantly declined by the mid-point of the drought treatment (12 h), to levels on par with, or even lower than, the untreated condition (Fig. 7A). After being treated with PEG for 72 h, *AsGSTU12*, *AsGSTU13*, and *AsGSTU15* were up-regulated about twofold, and *AsGSTU14* was up-regulated about fivefold (Fig. 7A).

Expression of AsGST under cadmium stress in *A. sativa*

To assess the function of *AsGST* genes in response to cadmium stress, we examined transcript abundance alterations of 118 *AsGST* genes in *A. sativa* leaves and roots under cadmium stress using transcriptome data (https://www.ncbi.nlm.nih.gov/bioproject/ PRJNA1116317) (Fig. 6C). In both root and leaf, 13 *AsGST* genes remained undetected. A total of 101 *AsGST* genes in leaves and 94 in roots displayed non-significant differential expression patterns as indicated in Table S7. As shown in Fig. 6D and 6E, four genes demonstrated significant expression differences in leaves and 11 in roots, respectively. Notably, *AsGSTU12*, *AsGSTU13*, *AsGSTU14*, and *AsGSTU15* displayed significant upregulation (4–13 folds) in both leaves and roots in response to cadmium treatment (Fig. 6D-E). To validate these results, we selected genes significantly upregulated in both roots and leaves (*AsGSTU12*, *AsGSTU13*, *AsGSTU14*, *AsGSTU15*), and assessed their expression using RT-qPCR across four time points (6 h, 12 h, 48 h, and 72 h). RT-qPCR results showed early up-regulation (within 12 h) in leaves of all four genes in response to cadmium treatment, but no significant difference or even suppression was detected afterward time points (Fig. 7C). In *A. sativa* roots, a transient up-regulation of four genes was observed, reaching a peak at 6 h of cadmium treatment, and then declining, with a 30-fold increase for *AsGSTU12*, 27-fold for *AsGSTU13*, 45-fold for *AsGSTU14*, and 20-fold for *AsGSTU15* (Fig. 7D). Although the RT-qPCR results showed varying degrees of up-regulation compared to the transcriptome data, the overall trend remained consistent.

Subcellular localization analysis of AsGSTU15 protein

To elucidate the expression pattern of GST proteins in *A. sativa*, the AsGSTU15 protein, with a significant response to both drought and cadmium stress, was chosen for the subcellular localization analysis. The AsGSTU15 fused with the green fluorescent protein (35S::AsGSTU15-GFP) was transformed in tobacco leaf,

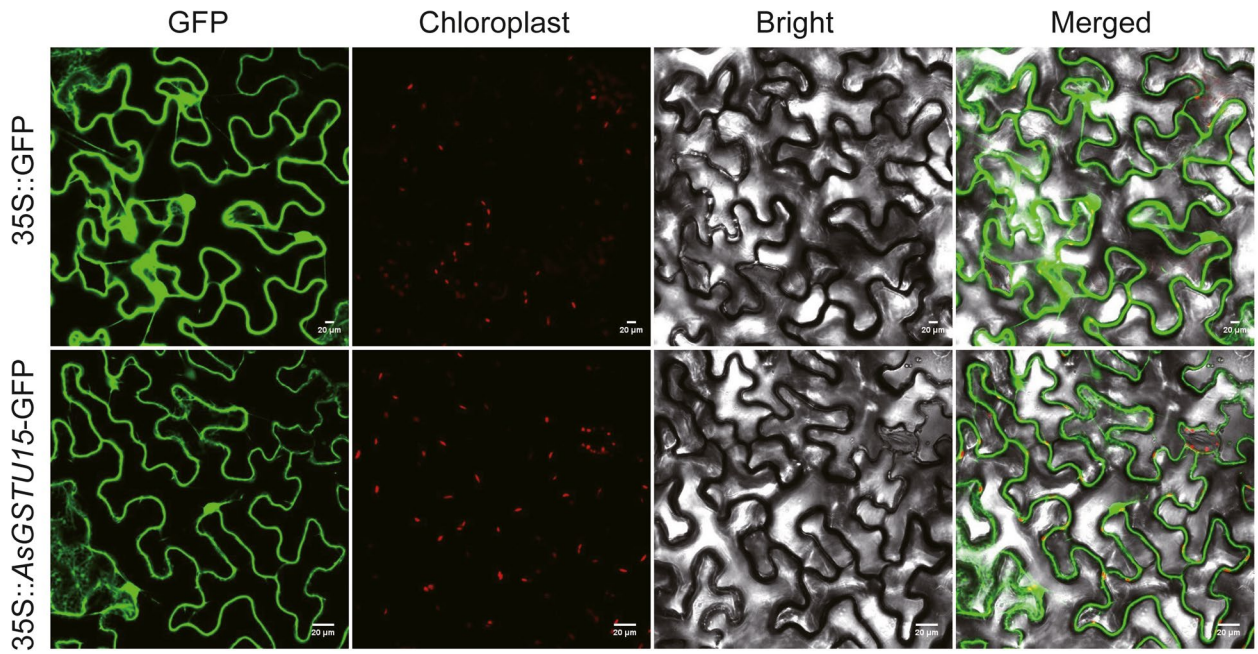

Fig. 8 Subcellular localization of AsGSTU15. Bars = 20 μm

and expressed in both cytoplasm and nucleus of tobacco epidermal cells, suggesting the localization of AsGSTU15 protein in these regions (Fig. 8). This finding aligns with the prediction of the Wolf website, which postulated the cytoplasmic localization of AsGSTU15 protein primarily (Table S4).

Upstream regulatory mechanism of AsGSTU gene and prediction of interacting proteins

To explore the regulatory mechanisms of *AsGSTU12*, *AsGSTU13*, *AsGSTU14*, and *AsGSTU15* genes in response to drought and cadmium stress, we postulated their potential upstream transcription factors (TFs) and interacting proteins. Utilizing transcriptome data from *A. sativa* roots under these stress conditions, we identified 394 common DEGs (Fig. 9A). From this differential gene set, a potential transcription factor regulatory network was conceived (Fig. 9B). Our analysis revealed six transcription factors that may potentially regulate these target genes. Notably, two genes from the *ERF* family, *AVESA.00010b.r2.2 CG0297950* and *AVESA.00010b.r2.2DG0331590*, demonstrated a high likelihood of binding to *AsGSTU15* and *AsGSTU12*, with their expression levels notably amplified under drought and cadmium stresses (Fig. 9D and E). These genes may act as key upstream transcription factors. Additionally, *AVESA.00010b.r2.3DG0552900* and *AVESA.00010b.r2.4 AG0632530* from the *NAC* transcription factor family, which also demonstrated elevated expression levels under the stress conditions, may exert some regulatory influence. The prediction of interacting proteins revealed that from the differential gene set, *AsGSTF58*, from the same *GST* gene family, had the closest interaction with the target genes and its expression level was amplified under stress conditions. This was followed by *AVESA.00010b. r2.1DG0134140*, which is homologous to *AtBGLU*, and *AVESA.00010b.r2.6 CG1099650* gene, homologous to *AtGER5*, both identified as potential interacting proteins for future examination.

Physiological response of *A. sativa* to drought and cadmium stress

To investigate the physiological responses of *A. sativa* to drought and cadmium stress, we analyzed dynamic changes in GSH content in shoots and roots under different stress durations (Fig. 10). Under drought stress (Fig. 10B, C), shoot GSH content increased significantly over time, reaching the highest at 48 h. In contrast, root

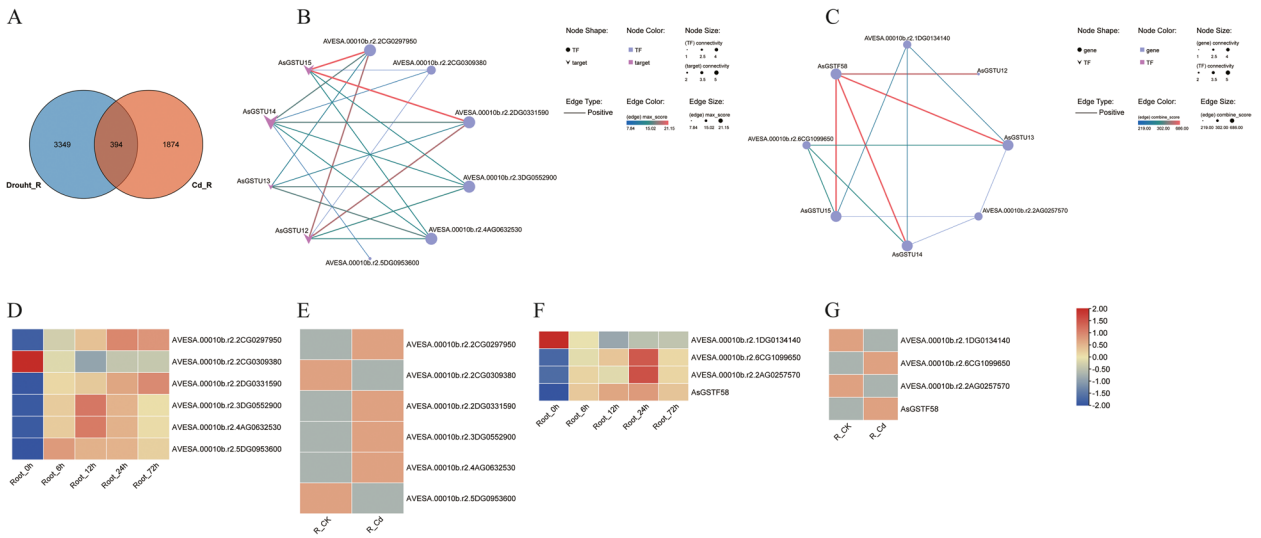

Fig. 9 Prediction of upstream transcription factors and interacting proteins for four differentially expressed genes, and the expression levels of different genes in the transcriptome under drought and cadmium stress. **A** Venn diagram of different genes in roots under cadmium and drought stress. The two gene sets are filled with different colors, and the overlapping area represents the genes shared between the gene sets, with numbers indicating the count of shared genes. **B**, **C** Prediction of upstream transcription factors and interacting proteins for the target genes. Nodes represent gene or protein names, with pink nodes indicating transcription factors. The size of the nodes represents gene connectivity, with larger nodes indicating stronger connectivity. Lines connecting nodes represent the interaction relationships between genes or proteins. The color of the lines (min p-value) represents the probability of motif occurrence or protein interaction, with smaller p-values indicating more reliable results. The thickness of the lines (max score) represents the motif occurrence score, with thicker lines indicating a higher possibility of transcription factor binding to the output sequence or stronger protein interaction. **D** A heatmap shows the expression profiles of six predicted transcription factors in roots under drought stress. **E** A heatmap shows the expression profiles of six predicted transcription factors in roots under cadmium stress. **F** A heatmap shows the expression profiles of four predicted interacting proteins in roots under drought stress. **G** A heatmap shows the expression profiles of four predicted interacting proteins in roots under cadmium stress

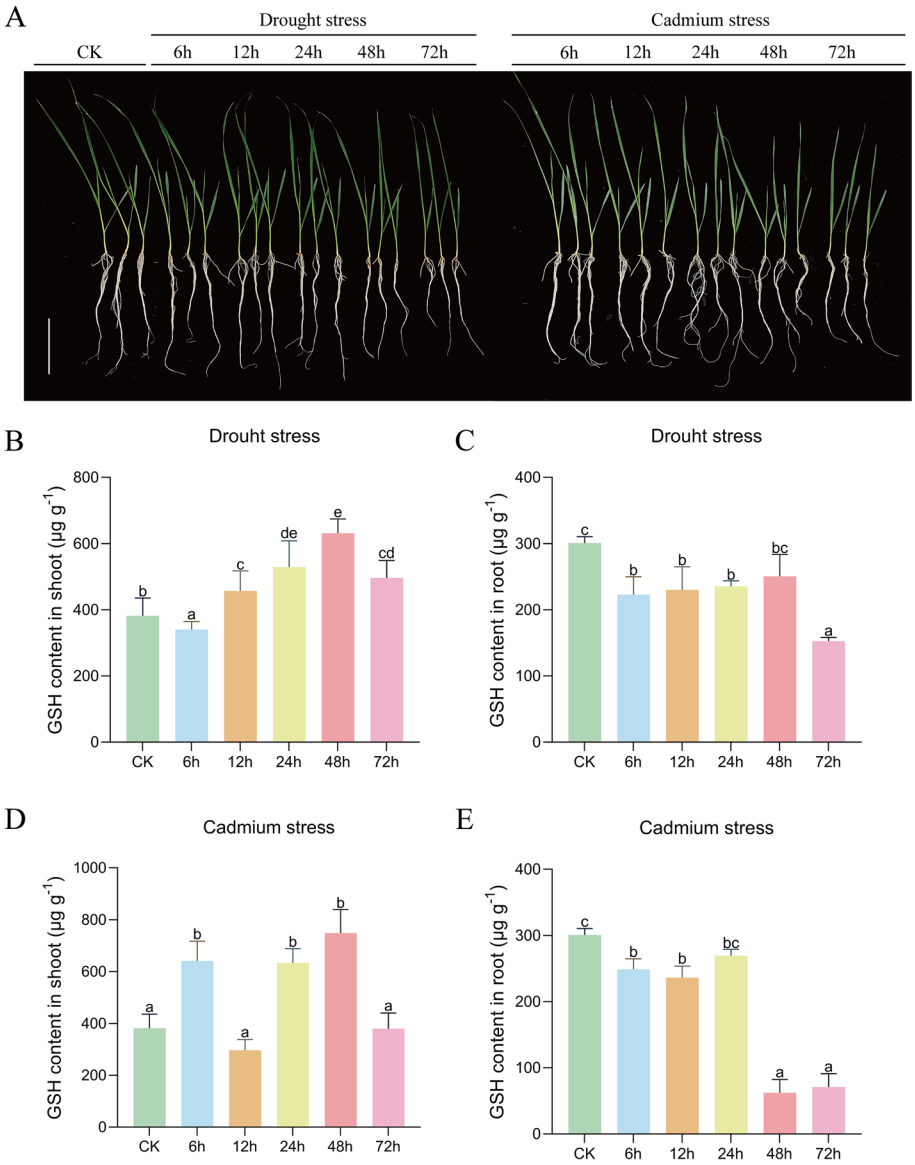

Fig. 10 Growth status and GSH content of *Avena sativa*. **A** The growth status of *A. sativa* at six time points (0–72 h); the scale bar is 10 cm. **B** The analysis results of GSH content. The mean ± standard deviation was obtained from six biological replicates. Error bars indicate the standard deviation. Different letters indicate significant differences, while the same letters indicate no significant differences at $P < 0.05$ level

GSH content decreased after an initial reduction at 6 h, with the lowest value at 72 h. Under cadmium stress, shoot GSH demonstrated an initial elevation at 6 h, followed by successive fluctuations characterized by a secondary peak at 48 h before declining to baseline levels at 72 h (Fig. 10D). This oscillatory response differed markedly from the consistent depletion observed in cadmium-stressed roots (Fig. 10E), where glutathione content exhibited progressive reduction from 6 h onward, maintaining persistently low concentrations through 48–72 h of treatment.

Discussion

The *GST* gene family, characterized by its multifunctionality, is ubiquitous in plant species and has gathered considerable interest due to its functional complexity. Comprehensive genome-wide analyses have been conducted across an array of plants, including *A. thaliana* [30], *O. sativa* [31], *S. lycopersicum* [32], *T. aestivum* [33], *Hordeum vulgare* [34], *G. hirsutum* [13], *Glycine max* [35], and *Solanum tuberosum* [36]. Notably, the sequencing of the *A. sativa* genome has

been successfully accomplished [28, 29], promoting advanced investigations into the function of the *GST* gene family.

Identification and bioinformatics analysis of the AsGST gene family

In our research, we conducted a thorough characterization of the *GST* gene family in *A. sativa*. The bioinformatic analysis identified 118 *AsGST* genes, classified into five distinct subfamilies: Tau, Phi, Zeta, Lambda, and EF1Bγ. This classification was based on the subfamily categorization in *A. thaliana* and *O. sativa*. Phylogenetic examinations revealed that the *AsGST* members closely resembled those of the same *GST* category in *A. thaliana* and *O. sativa*—a similarity that suggests a shared ancestral lineage. Interestingly, despite the considerable size of the *A. sativa* genome (10.76 Gb) [29], which is approximately 79.6 times larger than that of *A. thaliana* (135 Mb) [37] and about 40 times that of *O. sativa* (385.7 Mb) [38], the *AsGST* genes did not exhibit the Theta, DHAR, and TCHQD subfamilies observed in *A. thaliana* and *O. sativa*. This indicates that the *AsGST*'s evolutionary trajectory may involve gene loss or divergence, associated with functional substitution and environmental adaptation [39], and may not be directly influenced by genome size. Of all the identified classes, the Phi subfamily, with 59 members, was the largest in *A. sativa*, followed by the Tau subfamily with 40 members. This finding aligns with the widespread and distinct distribution of Tau and Phi subfamilies in plant species [40]. These genes have shown importance in plant response to various stresses, including salt [41], oxidative stress [42], heavy metal, and drought [43]. During species evolution, gene duplication is essential for the development of new biological functions and the expansion of gene families [42]. Gene family expansion is mainly realized by both segmental and tandem duplication [43]. Our research identified 108 segmental duplication pairs and 14 tandem duplication clusters unevenly distributed across the 21 chromosomes of the *AsGST* family, which are crucial for the evolution of the *AsGST* gene family. In this study, segmental duplication phenomena were predominantly observed, secondary to the role of tandem duplications, a trend similarly noted in the *GST* family of *T. aestivum* [43]. Moreover, the ka/ks ratios for all duplicated *AsGST* gene pairs were less than 1, suggesting that comprehensive purifying selection has occurred in all *AsGST* genes. This mechanism is likely critical for preserving gene functionality and promoting adaptability to environmental stressors.

The configuration of exon–intron structures is integral to gene evolution. Upon scrutinizing gene structures and conserved motifs, it was observed that varying *GST* types possess distinct motifs and gene structures. However, *AsGST* genes from the same subfamily display similarities in terms of exons and introns count and positioning, and they share comparable motifs. This finding implies potential expansive functional redundancy within the *AsGST* family, and suggests that *AsGST* genes from an identical subfamily may perform similar biological functions in *A. sativa*. Moreover, the number of exons/introns within *AsGST* family members ranged from zero to eleven, possibly indicative of deletion or insertion events throughout the evolutionary history of *A. sativa* [44].

Members of the *GST* family can respond to a broad spectrum of abiotic and biotic stresses. Regulatory elements known as cis-acting elements are integral to plant adaptation to these stresses, alongside growth and development, by controlling the expression of pertinent genes [45]. Analysis through PlantCARE revealed that the *AsGST* gene's promoter region encompasses three categories of cis-acting elements: those responsive to plant growth and development, abiotic and biotic stress, and phytohormone. These cis-acting elements may influence the expression level and response capability of *AsGST* family genes under various conditions such as growth, development, stress response, and hormone regulation. The results from the cis-acting element analysis suggest the potential involvement of *AsGST* genes in the regulation of *A. sativa* growth and development processes, such as seed, flower, and fruit development, and in responses to various abiotic and biotic stresses, which could include drought and heavy metal exposure. They may also be subject to regulation by hormones, such as abscisic acid and growth hormone, among others. The diverse array of cis-acting elements in the promoters of *AsGST* suggests potential synergistic interactions among the promoters, collectively enhancing the responsiveness of *AsGST* to a range of stimuli. This intricate regulatory network might enable *AsGST* to adapt flexibly to shifting environmental conditions, thus conferring stress (eg. drought and heavy metal) tolerance to *A. sativa*.

The predicted upstream TFs with the highest binding probability were *AVESA.00010b.r2.2 CG0297950* and *AVESA.00010b.r2.2DG0331590*, both belonging to the *ERF* family and functioning as ethylene response factors in plants. BLASTX analysis revealed that *AVESA.00010b.r2.2 CG0297950* is analogous to the *AtERF114*, which plays a crucial role in plant regeneration and development by regulating growth hormone signaling in response to mechanical and hormonal signals, thereby influencing the developmental and regenerative organ responses [46]. *AtERF114* also controls the synthesis of secondary metabolites by upregulating *AtPAL1* transcription, consequently enhancing resistance to fungal pathogens in *A. thaliana* [47]. *AVESA.00010b.r2.2DG0331590*, conversely, is analogous to *AtERF113*, which plays a significant role in

plant response to abiotic stresses. For instance, *GmERF113* was found to positively regulate drought response by activating *GmPR10 -1* expression, thereby improving plant drought resistance [48]. Moreover, *RhERF113*, induced by ethylene in floral organs and upregulated during flower senescence, can regulate cytokinin content during ethylene-induced petal senescence [49]. In *A. sativa*, these two genes may enhance plant tolerance to drought and cadmium stresses by regulating *AsGSTU12* or *AsGSTU15* expressions. Subcellular localization experiments indicated that the AsGSTU15 protein is located in both the cytoplasm and nucleus (Fig. 8), and given that transcription factors ordinarily function in the nucleus, *ERF* family transcription factors *AVESA.00010b.r2.2 CG0297950* and *AVESA.00010b.r2.2DG0331590* may regulate *AsGSTU15* expression in the nucleus. Protein interaction predictions showed that AsGSTF58 has the highest interaction probability with AsGSTU12, AsGSTU13, AsGSTU14, and AsGSTU15 (Fig. 9). Although these proteins belong to different GST subfamilies, their structural and functional similarities suggest joint participation in antioxidant response and heavy metal detoxification processes in response to drought and cadmium stresses. Subsequently, the proteins with the second highest binding probability were AVESA.00010b.r2.1DG0134140 and AVESA.00010b.r2.6 CG1099650. BLASTX comparison showed that *AVESA.00010b.r2.1DG0134140* is analogous to the *AtBGLU6*, a β-glucosidase gene of the glycoside hydrolase family 1 (*GH1*) involved in various biochemical processes [50]. In *O. sativa*, the *BGLU6* gene (*Os3BGlu6*) can hydrolyze glucose-bound ABA (ABA-GE) to free ABA, promoting stomatal closure, reducing water evaporation, and enhancing plant drought tolerance [51]. Additionally, *AVESA.00010b.r2.6 CG1099650* is homologous to the *AtGER5* gene, another ABA and stress response protein involved in ABA-mediated stress response. Increased ABA levels under abiotic stress conditions, such as drought, correspond to an upregulation of *AtGER5* expression, aiding plants in regulating their response to drought stress [52]. Hence, *AtBGLU6* and *AtGER5* homologs in *A. sativa* may functionally complement these four *AsGSTU* genes and synergistically participate in signaling and regulation, thereby enhancing plant tolerance to abiotic stress and exhibiting higher binding probability with target genes in the protein interaction network.

The AsGSTU subfamily may respond to PEG-induced drought stress by regulating redox homeostasis through scavenging ROS, participating in the ABA signaling pathway, and regulating osmotic homeostasis

Drought stress substantially impedes plant growth and crop yield, with the expression pattern of the *GST* gene family closely associated with plant resistance [32]. GSH is a critical regulator of cell growth and proliferation, with alterations in its content closely linked to a plant's physiological state [53]. The overexpression of *AtGST17* in *A. thaliana* led to a marked increase in the GSH/GSSG ratio and a greater accumulation of GSH and ABA, thereby regulating the intracellular redox balance, reducing stomatal aperture, lowering transpiration rates, and ultimately enhancing drought tolerance [54]. The primary sites for ROS production are chloroplasts and mitochondria within above-ground leaves [55], and GSH plays a crucial role in mitigating ROS damage [56]. For instance, overexpression of *PtrGSTU23* in *Populus trichocarpa* [57] and *CsGSTU8* in *A. thaliana* [18] reduced in vivo ROS content by catalyzing reactions between GSH and ROS, thereby improving drought tolerance. Under drought stress, in vivo ROS such as H_2O_2 content in *A. sativa* significantly accumulated, leading to a consequential rise in GST enzyme activity [58]. The present study found that *A. sativa* growth and development were markedly hindered under drought conditions (Fig. 10A), possibly due to the altered resource allocation under stress conditions, where resources were primarily used to manage drought stress instead of growth and development. Changes in *A. sativa*'s GSH content were intimately associated with its physiological status. Under drought stress, shoot GSH content in *A. sativa* significantly decreased in the initial stage (6 h), potentially due to the sharp increase in ROS levels at this time, using large amounts of GSH for ROS scavenging to protect cells from oxidative stress damage. Over time, the GSH content gradually increased, peaking at 48 h, suggesting that *A. sativa* may have initiated corresponding regulatory mechanisms, such as improving the antioxidant defense system and increasing the synthesis or recycling of GSH to maintain intracellular GSH homeostasis and more effectively manage persistent ROS stress. Despite a decrease at 72 h, the GSH content remained significantly higher than the control, indicating *A. sativa*'s strategy to maintain redox homeostasis under prolonged drought stress (Fig. 10B). Conversely, root GSH content progressively declined under drought stress, reaching a minimum at 72 h (Fig. 10C). This may suggest that roots experienced substantial inhibition under drought stress (Fig. 10A) and, as they are not the primary ROS-producing organ, may not require excessive GSH for ROS scavenging.

Transcriptome data analysis highlighted that 22 *AsGST* genes were markedly differentially expressed in *A. sativa* roots under drought treatment, most of which belonged to the Tau subfamily. Notably, four genes (*AsGSTU12*, *AsGSTU13*, *AsGSTU14*, and *AsGSTU15*) were significantly upregulated, with their transcript levels increasing approximately threefold under drought stress. The RT-qPCR validation results, consistent with the

transcriptome data, affirmed the positive role of these four genes in the drought stress response. BLASTX comparison revealed that *AsGSTU12* shared the highest homology with *AtGSTU15*, *AsGSTU13* and *AsGSTU15* with *AtGSTU17*, and *AsGSTU14* with *AtGSTU18*. No direct studies have elucidated the specific functions of *AtGSTU15* and *AtGSTU18* yet. The prediction of promoter cis-acting elements suggests that all four *AsGSTU* genes of *A. sativa* may contain ABRE elements (abscisic acid responsive elements), and it has been determined that *AtGSTU17* expression is induced by ABA, which negatively regulates plant drought tolerance [54]. Under drought conditions, *atgstu17* displayed a lower water loss rate and smaller stomatal opening compared to the wild type, demonstrating greater drought tolerance. Concurrently, *atgstu17* accumulated higher levels of GSH under normal growth conditions, aiding in maintaining cellular redox balance under adverse conditions [54]. Additionally, *AtGSTU17* is implicated in the expression of hypocotyl elongation, anthocyanin accumulation, and far-red light-mediated greening inhibition in *A. thaliana* seedlings, with its expression level regulated by various photoreceptors, especially photoreceptor phytochrome A (phyA), which functions under all light conditions [59]. Therefore, it is hypothesized that the *AsGSTU13* and *AsGSTU15* genes (homologous of *AtGSTU17*) may exhibit similar functions in response to drought stress in *A. sativa*. These genes may be both regulated by ABA signaling and express fluctuations in up- or down-regulation in *A. sativa* leaves and roots under different temporal drought treatments (Fig. 7A and B) controlling GSH content (Fig. 10B, C) for scavenging excess ROS to avert oxidative damage and ensure a basic level of ROS signaling function [58]. However, *AsGSTU12*, *AsGSTU13*, *AsGSTU14*, and *AsGSTU15* were upregulated in roots at various treatment times because roots are the first to sense drought and water deficit, and persist in these conditions. It is posited that the *GSTU* gene family effectively promotes the GSH-catalyzed detoxification to scavenge ROS and prevent root over-oxidization, hence the GSH content decreased (Fig. 10C). The *AtGSTU18*, homologous to *AsGSTU14*, has been shown to scavenge the reactive carbonyl compound acrolein (RCS) produced by ROS oxidizing the plasma membrane, thus mitigating the toxic effects of RCS on cells [60]. There are no known studies on the *AtGSTU15*, homologous to the *AsGSTU12*. However, its significant upregulated expression in *A. sativa* roots and transient expression in leaves may be similarly induced or regulated by ABA, as well as involved in ROS scavenging and signaling roles.

Osmoregulatory substances like proline and betaine are integral for preserving osmotic equilibrium and safeguarding cellular structure and function [61]. Notably, contents of these substances significantly escalated in *Nicotiana tabacum* with overexpressed *GSTU* gene under drought stress conditions [62]. Conversely, *osgstu17* displayed a significant reduction in leaf proline content, highlighting the crucial role of *OsGSTU17* in positively regulating proline synthesis [63]. Consequently, we conjecture that the four *AsGSTU* genes in *A. sativa* may contribute to osmotic regulation under PEG-induced drought stress, thereby maintaining intracellular osmotic pressure equilibrium and cellular membrane stability, and ultimately augmenting the plant's drought resilience.

The AsGSTU subfamily may respond to cadmium stress by regulating redox homeostasis through scavenging of ROS and promoting cadmium chelation and compartmentalization

Cadmium, an extremely toxic heavy metal pollutant, significantly disrupts plant growth and development. Unlike drought stress, cadmium exerts direct toxicity on plant cells, severely hampering *A. sativa* growth and development following cadmium treatment (Fig. 10A). Cadmium stress results in an excessive ROS accumulation, thus inducing oxidative stress. This process involves production and signal transduction of various substances, which cause oxidative damage to biomolecules (eg. proteins, lipids, and nucleic acids), subsequently affecting enzymatic activity and cellular membrane integrity [64]. The *GST* gene family is pivotally involved in plant response to cadmium stress. The GST enzyme, by facilitating the combination of GSH with the cadmium ion to form either non-toxic or less toxic complexes, diminishes cellular cadmium toxicity, promotes its detoxification and sequestration, and thus enhances plant tolerance to cadmium stress [65].

Under cadmium stress, the GSH content in the shoot of *A. sativa* exhibited a significant fluctuation, reflecting its role in ROS scavenging and cadmium ion chelation (Fig. 10D). At early stage of the cadmium stress (6 h), a substantial increase in GSH content occurred alongside the upregulation of *AsGSTU12*, *AsGSTU13*, and *AsGSTU15* expressions (Fig. 7C). GSH, functioning as a crucial antioxidant, rapidly scavenges excess ROS thereby mitigating cellular oxidative damage. Additionally, GSH forms stable complexes with cadmium ions, effectively immobilizing them within cells and/or transporting them to vesicles, thus reducing cytoplasmic cadmium ion concentration and preventing organellar damage caused by cadmium. However, as cadmium stress continues, GSH content fluctuates and corresponding *AsGSTU14* and *AsGSTU15* show differential upregulation (Fig. 7C). This response likely reflects a balance of ongoing ROS scavenging, maintenance of a certain ROS level for signaling

purposes, and compartmentalization of cadmium ions facilitating sustained, albeit slow, growth and development (Fig. 10A). Similarly, *Cosmos bipinnatus* enhances cadmium tolerance via the augmentation of antioxidant levels attributed to an increase in GSH content [66]. *O. sativa* strains that overexpress the *OsGST* (*LOC_Os10 g38160*) gene display augmented cadmium resilience and diminished cadmium accretion, inferring that the *OsGST* gene modulates cadmium accumulation and resistance in rice through the preservation of redox equilibrium [67]. It has also been observed that overexpression of either *OsGSTU5* or *OsGSTU37* lines significantly elevated GSH content and enhanced seed germination, seedling growth, and survival under cadmium-related stress [65]. Consistent with this, overexpressing of *OsGSTU6* resulted in a decreased cadmium accumulation in foliage, thereby boosting plant tolerance to cadmium-induced stress [68]. Conversely, under cadmium stress, the GSH content in *A. sativa* roots decreases, reaching a nadir at 48–72 h (Fig. 10E). This decrease likely reflects cadmium-induced metabolic disruption in roots, where GSH is prioritized for ROS scavenging and cadmium chelation. Despite the depletion of GSH, *GSTU* family genes (*AsGSTU12*, *AsGSTU13*, *AsGSTU14*, and *AsGSTU15*) were upregulated after 6 h of cadmium treatment, with most exhibiting significantly higher expression levels than controls at subsequent time points. This suggests that the heavy consumption of GSH for ROS scavenging and continual cadmium ion chelation depletes GSH content, and potentially inhibits the activity and gene expression of enzymes crucial to GSH synthesis and metabolism. Overexpression of *PuGSTU17* enhances resistance to Zn^{2+} stress by increasing root GST content and reducing H_2O_2 content [69]. The expression profile of *GSTU* family genes in different parts of the plant over time reinforces their role in ROS scavenging and cadmium ion binding, underscoring their critical function in *A. sativa*'s resistance to heavy metal cadmium.

Conclusions

In this study, an in-depth investigation was conducted on the composition, structure, and stress responses of the *AsGST* gene family. Bioinformatic analysis identified 118 *AsGST* genes grouped into five subfamilies, which exhibited significant fluctuation in their expression patterns under adverse stress. Notably, four genes within the Tau subfamily (*AsGSTU12*, *AsGSTU13*, *AsGSTU14*, and *AsGSTU15*) demonstrated significant upregulation under both drought and cadmium stress. It was postulated that these four *AsGSTU* genes contribute towards the catalytic scavenging of ROS via GSH substrates, thus regulating redox equilibrium and maintaining basic ROS signaling roles. Under cadmium stress, these genes are hypothesized to respond by facilitating the scavenging of ROS using GSH to regulate redox homeostasis, promoting the chelation and fixation of GSH with cadmium, or by compartmentalizing cadmium under heavy metal stress. This study revealed the conjoint effects of these four *AsGSTU* genes under drought and cadmium stress, offering valuable genetic resources for *A. sativa* stress tolerance breeding and adversity adaptation research.

Materials and methods

Identification and classification of GST genes from A. sativa

In this research, the genome and annotation data of *A. sativa* were procured from the GrainGenes database (https://wheat.pw.usda.gov/GG3/content/avena-sang-download). Concurrently, the protein sequences of 53 AtGST (Table S1) were retrieved from the TAIR database (https://www.arabidopsis.org/) [30]. From the Ensembl plant database (http://plants.ensembl.org/index.html), we obtained the protein sequences of 77 OsGST (Table S2), although the protein sequences for OsGSTU3 (LOC_Os10 g38501) and OsGSTU4 (LOC_Os10 g38495) were not found [31]. These 130 assembled sequences were utilized as reference protein sequences for a BLASTP search employing TBtools-II software (version 2.119) [70], with an E-value $\leq 1e^{-10}$ and identity $\geq 50\%$ as screening criteria, to identify *GST* genes in *A. sativa* [71]. The subsequent screening of the potential *AsGST* genes was performed using HMMER software (version 3.0), applying the Hidden Markov Model (HMM) of characteristics of GST-N (PF02798) and GST-C (PF00043) structural domains from the PFAM database (https://pfam-legacy.xfam.org/), with an E-value threshold set at $<1 \times 10\text{^}{-5}$. Redundant sequences from these protein sequences were removed using CD-HIT (version 4.8.1) with parameters set at c = 0.9 and n = 5. Only the longest transcripts were selected for *AsGST* genes with multiple transcripts [72]. The integrity of conserved structural domains in the protein sequences of candidate genes was examined using the NCBI conserved domain database (https://www.ncbi.nlm.nih.gov/cdd/) and the Simple Modular Architecture Research Tool (SMART) website (https://smart.embl.de/), discarding those potential genes not containing GST-conserved structural domains. Physicochemical properties of AsGST proteins, including protein length, molecular weight, isoelectric point, instability index, and average hydrophobicity, were analyzed via the ExPASy-ProtParam website (https://www.expasy.org/resources/protparam) [73]. Predictions of the subcellular localization of the AsGST were made using the WOLF PSORT website (https://wolfpsort.hgc.jp/).

Chromosome localization and phylogenetic tree construction

Utilizing TBtools-II software gene localization visualization tool, we ascertained the chromosomal locations of different *AsGST* gene classes using annotation data from *A. sativa* [70]. To delve into the phylogenetic relationships and evolutionary history of *AsGST* genes, we amalgamated the identified AsGST proteins with 150 GST proteins from *A. thaliana* and *O. sativa* referenced in prior studies. This was followed by a multiple sequence comparison using the default parameters of Clustal X software. Based on the categorization of *A. thaliana* and *O. sativa* subfamilies in the sequence comparison results and the structural features of AsGST proteins, we classified and named the *AsGST* genes. In *A. sativa*, gene names commence with the prefix "As" followed by a category identifier. Hence, the *AsGST* genes were ultimately sorted into five subfamilies: *AsGSTU*, *AsGSTF*, *AsGSTZ*, *AsGSTL*, and *AsEF1BG*, representing the Tau, Phi, Zeta, Lambda, and EF1Bγ subfamilies, respectively [74, 75]. Lastly, we constructed a neighbor-joining phylogenetic tree encompassing all these genes using MEGA software (version 11.0) and employed the Interactive Tree of Life (iTOL) website (https://itol.embl.de/) for phylogenetic tree refinement.

Analysis of the conserved domain and gene structure

We conducted a conserved motif analysis of AsGST proteins using the MEME online platform (https://meme-suite.org/meme/). In this analysis, we aimed to identify 10 conserved motifs, keeping other parameters at default settings. Following this, we inputted the phylogenetic tree file, conserved motif information, genome annotation data, and the protein structure domain prediction file derived from the NCBI-CDD tool (https://www.ncbi.nlm.nih.gov/cdd/) into the gene structure view component of the TBtools-II software. This comprehensive procedure facilitated the visualization and analysis of the phylogenetic tree, conserved motifs, structural domains, and gene structures of *AsGST* genes.

Cis-acting element analysis of AsGST promoter region

Utilizing the annotation file of *A. sativa*, sequences 2000 bp upstream of the start codon of the *AsGST* gene were procured through the GTF/GFF3 sequence extraction instrument of TBtools-II. These sequences underwent analysis using the PlantCARE database (https://bioinformatics.psb.ugent.be/webtools/plantcare/html/) to discern cis-acting elements within the promoter region of the *AsGST* gene. Subsequently, the promoter region of the *AsGST* gene underwent visualization and enumeration of the cis-acting elements within its promoter region by use of the Simple BioSequence Viewer tool of TBtools-II. The fresh data were then collated and displayed in Excel for further scrutiny.

Analysis of gene duplication and collinearity

We employed the One Step MCScanX tool within TBtools-II software, setting the E-value limit below $1\times 10^{\wedge -10}$, to identify *AsGST* gene duplication events. The Advance Circos program was subsequently used to visualize and analyze the location, gene density, and covariance details of the *AsGST* gene. Concurrently, we employed multiple covariate scanning methods to further identify homologous genetic linkages within the *A. sativa* genome and across other species. Additionally, the Simple Ka/Ks Calculator tool in TBtools-II software was utilized to calculate the ratio of non-synonymous to synonymous mutation rates (Ka/Ks) for two protein-coding genes, which is a pivotal determinant for the selection pressure on the genes.

Plant material and stress treatment

A. sativa seeds were initially screened using a crop seed tester (BIO-seed M-P, Research Center of Information Technology, Beijing Academy of Agriculture and Forestry Sciences, Beijing, China) based on the length, width, and perimeter of the seeds. The seeds then underwent sterilization via a 20-min immersion in a 1.5% sodium hypochlorite solution, prior to being relocated to germination boxes. *A. sativa* seedlings were grown in a light-shielded growth chamber at a stable temperature of 25 ± 1 °C until attaining a height between 2–3 cm. Seedlings were then transferred to the two-true leaf phase in a 1/2 Hoagland nutrient solution that contained either 15% (w/v) polyethylene glycol 6000 (PEG 6000) or 100 μM $CdCl_2$ for subsequent treatment. Following different treatment durations at 0 h, 6 h, 12 h, 24 h, 48 h, and 72 h, samples were collected. The shoot and root portions of plants were cleansed with sterile water, excess water was eliminated, and they were quickly frozen using liquid nitrogen. The samples were then preserved at − 80 °C in a refrigerator for future experimental analysis.

RNA extraction and RT-qPCR

Total RNA extraction from the leaves and roots of *A. sativa* was conducted at each time point utilizing an RNAiso Plus kit (Takara, Japan) as per the kit's user manual. Subsequently, Nanodrop spectrometry (Thermo Fisher Scientific, USA) was employed to ascertain the concentration and purity of the total RNA. The PrimeScript™ RT kit (Takara, Japan) was then used to synthesize first-strand complementary DNA (cDNA), using 1 μg of total RNA as a template. Furthermore, primer design for RT-qPCR experiments (Table S3) was executed using Primer Premier software (version 5.0), and primer

specificity was confirmed using the Primer Check function of TBtools-II software. RT-qPCR assays were carried out using the CFX Connect instrument (Bio-Rad, USA) and ArtiCan^{CEO} SYBR qPCR Mix reagents (Tsingke, China). The total reaction system was set to a volume of 20 μL, comprising 10 μL of ArtiCan^{CEO} SYBR qPCR Mix, 0.4 μL each of upstream and downstream primers (at 10 μM concentration), and 2 μL of template cDNA, diluted tenfold with water. The remaining volume was topped up to 20 μL with ddH_2O. The RT-qPCR reaction parameters were as follows: Pre-denaturation at 95 °C for 5 min, followed by denaturation at 95 °C for 10 s, and annealing at 60 °C for 30 s, with a total of 40 cycles. The default values of the instrument were used for the melting curve acquisition program. The internal reference gene GAPDH was used to normalize cDNA concentration [76]. Lastly, the relative gene expression levels were determined using the $2^{-\Delta\Delta CT}$ method [77].

Subcellular localization

We integrated the CDS of the *AsGSTU15* gene, which lacks a stop codon, into the 35S::GFP binary vector based on pBWA(V)HS via molecular cloning techniques. Then we electroporated the constructed plasmid into the GV3101 strain of Agrobacterium. Following electro-transformation, the Agrobacterium culture was incubated at 30 °C for a two-day period before being transferred to a kanamycin-containing YEB liquid medium to extend the incubation process. After an hour-long incubation at 28 °C in a shaking environment of 170 rpm, centrifugation at 4000 rpm for 4 min removed the supernatant. The organisms were then resuspended in a solution comprising 10 mM $MgCl_2$ and 120 μM acetylsulfate (AS), and the OD600 value of the bacterial solution was adjusted to approximately 0.6. Healthy *N. tabacum* plants were selected for infiltration with the bacterial solution through the lower epidermis of the leaves, using a needleless 1 mL syringe. Post injection, the *N. tabacum* plants were cultivated in low-light conditions for two days. Subsequently, slides were prepared from the leave's injection site to detect the GFP fluorescence signal using a laser confocal microscope (Nikon C2-ER Confocal Microscope, Tokyo, Japan).

Physiological analysis

Three *A. sativa* plants per treatment group were randomly selected for phenotypic observations to evaluate the effects of different treatments and time points on growth. All observations were conducted under uniform light and background conditions to ensure comparability of results. Images of the *A. sativa* plants were captured from both front and side angles to document morphological changes. Additionally, six *A. sativa* plants from each treatment group were randomly selected, their fresh leaf tissues collected and then promptly frozen in liquid nitrogen for the subsequent analysis. The GSH content was determined in shoots and roots using a GSH content assay kit (Solarbio, China). The procedure involved homogenizing 0.1 g of *A. sativa* tissue in 1 mL of Reagent 1, disrupting the tissue with a TissueLyser II (QIAGEN, Germany), followed by the addition of multiple reagents, with absorbance measured at 412 nm.

Prediction of upstream transcription factors and interacting proteins

Transcriptome analysis of *A. sativa* roots under drought and cadmium stress was performed utilizing the VennDiagram and UpSetR packages in R to create Venn diagrams and identify genes common to both differential gene sets. The motif information for transcription factor binding was then assessed from the JASPAR database (http://jaspar.genereg.net) for these shared differential genes and predicted transcriptional target genes using MEME FIMO software (version 5.5.6). Subsequently, we mapped the network of potential transcription factor interactions associated with these target genes. Additionally, we analyzed the target protein interaction networks through the STRING protein interactions database (http://string-db.org). The BLASTX was employed to compare the sequences in the target gene set against the protein sequences of reference species within the STRING database, such as *A. thaliana* and *O. sativa*, thereby constructing the interaction network based on the protein interactions of these reference species.

Statistical analysis

Figures were generated using GraphPad Prism software (version 9.0.0), with data presented as mean values and corresponding standard deviations. Statistical analyses were conducted using IBM SPSS Statistics (version 26.0). To ensure the robustness of the experimental results, three biological replicates were conducted for each treatment group in the RT-qPCR experiments, while six biological replicates were performed for each treatment group in the GSH content determination experiments. Significance of the data was assessed using one-way analysis of variance (ANOVA), with a p-value threshold of less than 0.05 established for determining statistical significance.

Supplementary Information

The online version contains supplementary material available at https://doi.org/10.1186/s12870-025-06559-x.

Supplementary Material 1

Supplementary Material 2

Acknowledgements
Not applicable

Authors' contributions
CX, LJ and AL conceived and designed the research. BL and PH guided the experiment. CX and LJ conducted the experiments. CX and PH wrote the manuscript. JM, PY, JL, CL, YC, HZ, HAIA, QG and LS provided technical assistance. PY and SS critically reviewed and revised the manuscript. All authors have read and agreed to the published version of the manuscript.

Funding
This study was supported by the Guangdong Provincial Key Areas R&D Programs (2022B0202110003).

Data availability
All RNA-Seq data were deposited in the NCBI SRA database under the project PRJNA1056521 (https://www.ncbi.nlm.nih.gov/bioproject/PRJNA1056521) and the project PRJNA1116317 (https://www.ncbi.nlm.nih.gov/bioproject/PRJNA1116317).

Declarations

Ethics approval and consent to participate
Not applicable.

Consent for publication
Not applicable.

Competing interests
The authors declare no competing interests.

Author details
[1]Center of Information Technology, Beijing Academy of Agriculture and Forestry Sciences, Beijing 100083, China. [2]Research Center of Intelligent Equipment, Beijing Academy of Agriculture and Forestry Sciences, Beijing 100083, China. [3]State Key Laboratory of Nutrient Use and Management, College of Resources and Environmental Sciences, National Academy of Agriculture Green Development, China Agricultural University, Beijing 100193, China. [4]School of Biological Sciences, University of Western Australia, Crawley, WA 6009, Australia. [5]International Research Centre for Environmental Membrane Biology, Foshan University, Foshan 528000, China. [6]Department of Botany, Faculty of Science, Port Said University, Port Said 42526, Egypt. [7]College of Life Sciences, Laboratory of Plant Stress Responses and Related Gene Mining, Capital Normal University, Beijing 100048, China. [8]AgChip Science & Technology (Beijing) Co, Ltd, Beijing 100083, China.

Received: 24 February 2025 Accepted: 15 April 2025
Published online: 25 April 2025

References

1. Basantani M, Srivastava A, Sen S. Elevated antioxidant response and induction of tau-class glutathione S-transferase after glyphosate treatment in *Vigna radiata (L.) Wilczek*. Pest Biochem Physiol. 2011;99(1):111–7.
2. Dixon DP, Edwards R. Glutathione transferases The arabidopsis book. 2010;8: e0131.
3. Mohsenzadeh S, Esmaeili M, Moosavi F, Shahrtash M, Saffari B, Mohabatkar H. Plant glutathione S-transferase classification, structure and evolution. Afr J Biotechnol. 2011;10(42):8160–5.
4. Ahmad MZ, Nasir JA, Ahmed S, Ahmad B, Sana A, Salman S, Shah Z, Yang C. Genome-wide analysis of glutathione S-transferase gene family in *G. max*. Biologia. 2020;75:1691–705.
5. Edwards R, Dixon DP. Plant glutathione transferases. Methods Enzymol. 2005;401:169–86.
6. Sylvestre-Gonon E, Law SR, Schwartz M, Robe K, Keech O, Didierjean C, Dubos C, Rouhier N, Hecker A. Functional, structural and biochemical features of plant serinyl-glutathione transferases. Front Plant Sci. 2019;10:608.
7. Islam S, Rahman IA, Islam T, Ghosh A. Genome-wide identification and expression analysis of glutathione S-transferase gene family in tomato: gaining an insight to their physiological and stress-specific roles. PLoS ONE. 2017;12(11): e0187504.
8. Munyampundu J-P, Xu Y-P, Cai X-Z. Phi class of glutathione S-transferase gene superfamily widely exists in nonplant taxonomic groups. Evol Bioinform. 2016;12:EBO-S35909.
9. Ma L, Zhang Y, Meng Q, Shi F, Liu J, Li Y. Molecular cloning, identification of GSTs family in sunflower and their regulatory roles in biotic and abiotic stress. World J Microbiol Biotechnol. 2018;34:1–12.
10. Csiszár J, Horváth E, Váry Z, Gallé Á, Bela K, Brunner S, Tari I. Glutathione transferase supergene family in tomato: salt stress-regulated expression of representative genes from distinct GST classes in plants primed with salicylic acid. Plant Physiol Biochem. 2014;78:15–26.
11. Li B, Zhang X, Duan R, Han C, Yang J, Wang L, Wang S, Su Y, Wang L, Dong Y. Genomic analysis of the glutathione S-transferase family in pear (*Pyrus communis*) and functional identification of *PcGST57* in anthocyanin accumulation. Intern J Mol Sci. 2022;23(2):746.
12. Yang Q, Han XM, Gu JK, Liu YJ, Yang MJ, Zeng QY. Functional and structural profiles of GST gene family from three *Populus* species reveal the sequence–function decoupling of orthologous genes. New Phytol. 2019;221(2):1060–73.
13. Dong Y, Li C, Zhang Y, He Q, Daud MK, Chen J, Zhu S. Glutathione S-transferase gene family in *Gossypium raimondii* and *G. arboreum*: comparative genomic study and their expression under salt stress. Front Plant Sci. 2016;7:139.
14. Yuan L, Dang J, Zhang J, Wang L, Zheng H, Li G, Li J, Zhou F, Khan A, Zhang Z, et al. A glutathione S-transferase regulates lignin biosynthesis and enhances salt tolerance in tomato. Plant Physiol. 2024;196(4):2989–3006.
15. Gao H, Yu C, Liu R, Li X, Huang H, Wang X, Zhang C, Jiang N, Li X, Cheng S. The glutathione s-transferase *PtGSTF1* improves biomass production and salt tolerance through regulating xylem cell proliferation, ion homeostasis and reactive oxygen species scavenging in Poplar. Intern J Mol Sci. 2022;23(19):11288.
16. Yang G, Xu Z, Peng S, Sun Y, Jia C, Zhai M. In planta characterization of a tau class glutathione S-transferase gene from *Juglans regia* (*JrGSTTau1*) involved in chilling tolerance. Plant Cell Rep. 2016;35:681–92.
17. Zhao W-S, Yan L-F, Hu K-D, Zhou Z-L, Wang S-Q, Yan L-Y, Hu F, Zhang H, Yao G-F. Transcriptomic mechanism revealed *IbGST4* and *IbGST2* genes response to low-temperature stress in sweet potatoes. Postharvest Biol Technol. 2024;212: 112909.
18. Zhang Y, He J, Xiao Y, Zhang Y, Liu Y, Wan S, Liu L, Dong Y, Liu H, Yu Y. *CsGSTU8*, a glutathione S-transferase from *Camellia sinensis*, is regulated by *CsWRKY48* and plays a positive role in drought tolerance. Front Plant Sci. 2021;12: 795919.
19. Dixit V, Pandey V, Shyam R. Differential antioxidative responses to cadmium in roots and leaves of pea (*Pisum sativum* L. cv. Azad). J Exp Bot. 2001;52(358):1101–9.
20. Sharma R, Sahoo A, Devendran R, Jain M. Over-expression of a rice tau class glutathione s-transferase gene improves tolerance to salinity and oxidative stresses in *Arabidopsis*. PLoS ONE. 2014;9(3): e92900.
21. Srivastava D, Verma G, Chauhan AS, Pande V, Chakrabarty D. Rice (*Oryza sativa* L.) tau class glutathione S-transferase (*OsGSTU30*) overexpression in *Arabidopsis thaliana* modulates a regulatory network leading to heavy metal and drought stress tolerance. Metallomics. 2019;11(2):375–89.
22. Bräutigam M, Lindlöf A, Zakhrabekova S, Gharti-Chhetri G, Olsson B, Olsson O. Generation and analysis of 9792 EST sequences from cold acclimated oat. Avena sativa BMC Plant Biol. 2005;5:1–17.
23. Rasane P, Jha A, Sabikhi L, Kumar A, Unnikrishnan VS. Nutritional advantages of oats and opportunities for its processing as value added foods-a review. J Food Sci Technol. 2015;52:662–75.
24. Fu J, Zhang Y, Hu Y, Zhao G, Tang Y, Zou L. Concise review. Coarse cereals exert multiple beneficial effects on human health. Food Chem. 2020;325:126761.
25. Marshall A, Cowan S, Edwards S, Griffiths I, Howarth C, Langdon T, White E. Crops that feed the world 9. Oats-a cereal crop for human and livestock feed with industrial applications. Food Sec. 2013;5:13–33.
26. Ergashovich K, Tokhirovna J. Ecophysiological properties of white oats. In: Proceedings of the International Conference on Innovations in Sciences, Education and Humanities, Rome, Italy: 2021.

27. Mª Jesús Gutiérrez G, Jesús Pastor P, Ana Jesús H. Effect of Heavy Metals from Mine Soils on *Avena Sativa* L.and Education Strategies. In.: Parlar Scientific Publications; 2010.
28. Kamal N, Tsardakas Renhuldt N, Bentzer J, Gundlach H, Haberer G, Juhász A, Lux T, Bose U, Tye-Din JA, Lang D. The mosaic oat genome gives insights into a uniquely healthy cereal crop. Nature. 2022;606(7912):113–9.
29. Peng Y, Yan H, Guo L, Deng C, Wang C, Wang Y, Kang L, Zhou P, Yu K, Dong X. Reference genome assemblies reveal the origin and evolution of allohexaploid oat. Nat Genet. 2022;54(8):1248–58.
30. Sappl PG, Oñate-Sánchez L, Singh KB, Millar AH. Proteomic analysis of glutathione S-transferases of *Arabidopsis thaliana* reveals differential salicylic acid-induced expression of the plant-specific phi and tau classes. Plant Mol Biol. 2004;54:205–19.
31. Jain M, Ghanashyam C, Bhattacharjee A. Comprehensive expression analysis suggests overlapping and specific roles of rice glutathione S-transferase genes during development and stress responses. BMC Genomics. 2010;11:1–17.
32. Islam S, Sajib SD, Jui ZS, Arabia S, Islam T, Ghosh A. Genome-wide identification of glutathione S-transferase gene family in pepper, its classification, and expression profiling under different anatomical and environmental conditions. Scient Rep. 2019;9(1):9101.
33. Hao Y, Xu S, Lyu Z, Wang H, Kong L, Sun S. Comparative Analysis of the Glutathione S-Transferase Gene Family of Four *Triticeae* Species and Transcriptome Analysis of GST Genes in Common Wheat Responding to Salt Stress. Intern J Genomics. 2021;2021(1):6289174.
34. Rezaei MK, Shobbar Z-S, Shahbazi M, Abedini R, Zare S. Glutathione S-transferase (GST) family in barley: identification of members, enzyme activity, and gene expression pattern. J Plant Physiol. 2013;170(14):1277–84.
35. Liu H-J, Tang Z-X, Han X-M, Yang Z-L, Zhang F-M, Yang H-L, Liu Y-J, Zeng Q-Y. Divergence in enzymatic activities in the soybean GST supergene family provides new insight into the evolutionary dynamics of whole-genome duplicates. Mol Biol Evol. 2015;32(11):2844–59.
36. Ding N, Wang A, Zhang X, Wu Y, Wang R, Cui H, Huang R, Luo Y. Identification and analysis of glutathione S-transferase gene family in sweet potato reveal divergent GST-mediated networks in aboveground and underground tissues in response to abiotic stresses. BMC Plant Biol. 2017;17:1–15.
37. Arabidopsis Genome Initiative genomeanalysis@ tgr. org genomeanalysis@ gsf d. Analysis of the genome sequence of the flowering plant Arabidopsis thaliana. Nature. 2000;408(6814):796–815.
38. Shang L, He W, Wang T, Yang Y, Xu Q, Zhao X, Yang L, Zhang H, Li X, Lv Y. A complete assembly of the rice Nipponbare reference genome. Mol Plant. 2023;16(8):1232–6.
39. Jia J-S, Ge N, Wang Q-Y, Zhao L-T, Chen C, Chen J-W. Genome-wide identification and characterization of members of the LEA gene family in *Panax notoginseng* and their transcriptional responses to dehydration of recalcitrant seeds. BMC Genomics. 2023;24(1):126.
40. Frova C. The plant glutathione transferase gene family. Genomic structure, functions, expression and evolution. Physiol Plantarum. 2003;119(4):469–79.
41. Jha B, Sharma A, Mishra A. Expression of *SbGSTU* (tau class glutathione S-transferase) gene isolated from *Salicornia brachiata* in tobacco for salt tolerance. Mol Biol Rep. 2011;38:4823–32.
42. Hurles M. Gene duplication. The genomic trade in spare parts. PLoS Biol. 2004;2(7):e206.
43. Wang R, Ma J, Zhang Q, Wu C, Zhao H, Wu Y, Yang G, He G. Genome-wide identification and expression profiling of glutathione transferase gene family under multiple stresses and hormone treatments in wheat (*Triticum aestivum* L.). BMC Genomics. 2019;20:1–15.
44. Xu G, Guo C, Shan H, Kong H. Divergence of duplicate genes in exon–intron structure. Proc Natl Acad Sci. 2012;109(4):1187–92.
45. Narusaka Y, Nakashima K, Shinwari ZK, Sakuma Y, Furihata T, Abe H, Narusaka M, Shinozaki K, Yamaguchi-Shinozaki K. Interaction between two cis-acting elements, ABRE and DRE, in ABA-dependent expression of *Arabidopsis rd29A* gene in response to dehydration and high-salinity stresses. Plant J. 2003;34(2):137–48.
46. Canher B, Lanssens F, Zhang A, Bisht A, Mazumdar S, Heyman J, Wolf S, Melnyk CW, De Veylder L. The regeneration factors *ERF114* and *ERF115* regulate auxin-mediated lateral root development in response to mechanical cues. Mol Plant. 2022;15(10):1543–57.
47. Li Z, Zhang Y, Ren J, Jia F, Zeng H, Li G, Yang X. Ethylene-responsive factor *ERF114* mediates fungal pathogen effector PevD1-induced disease resistance in *Arabidopsis thaliana*. Mol Plant Pathol. 2022;23(6):819–31.
48. Fang X, Ma J, Guo F, Qi D, Zhao M, Zhang C, Wang L, Song B, Liu S, He S. The AP2/ERF *GmERF113* positively regulates the drought response by activating *GmPR10-1* in soybean. Intern J Mol Sci. 2022;23(15):8159.
49. Khaskheli AJ, Ahmed W, Ma C, Zhang S, Liu Y, Li Y, Zhou X, Gao J. *RhERF113* functions in ethylene-induced petal senescence by modulating cytokinin content in rose. Plant Cell Physiol. 2018;59(12):2442–51.
50. Miyahara T, Matsuba Y, Ozeki Y, Sasaki N. Identification of genes in *Arabidopsis thaliana* with homology to a novel acyl-glucose dependent glucosyltransferase of carnations. Plant biotechnol. 2011;28(3):311–5.
51. Wang C, Chen S, Dong Y, Ren R, Chen D, Chen X. Chloroplastic *Os3BGlu6* contributes significantly to cellular ABA pools and impacts drought tolerance and photosynthesis in rice. New Phytol. 2020;226(4):1042–54.
52. Baron KN, Schroeder DF, Stasolla C. GEm-Related 5 (GER5), an ABA and stress-responsive GRAM domain protein regulating seed development and inflorescence architecture. Plant Sci. 2014;223:153–66.
53. Koprivova A, Mugford ST, Kopriva S. *Arabidopsis* root growth dependence on glutathione is linked to auxin transport. Plant Cell Rep. 2010;29:1157–67.
54. Chen J-H, Jiang H-W, Hsieh E-J, Chen H-Y, Chien C-T, Hsieh H-L, Lin T-P. Drought and salt stress tolerance of an Arabidopsis glutathione S-transferase U17 knockout mutant are attributed to the combined effect of glutathione and abscisic acid. Plant Physiol. 2012;158(1):340–51.
55. Zhao Y, Yu H, Zhou J-M, Smith SM, Li J. Malate circulation: linking chloroplast metabolism to mitochondrial ROS. Trends Plant Sci. 2020;25(5):446–54.
56. Gill SS, Tuteja N. Reactive oxygen species and antioxidant machinery in abiotic stress tolerance in crop plants. Plant Physiol Biochem. 2010;48(12):909–30.
57. Niu MX, Feng CH, He F, Zhang H, Bao Y, Liu SJ, Liu X, Su Y, Liu C, Wang HL. The miR6445-*NAC029* module regulates drought tolerance by regulating the expression of glutathione S-transferase U23 and reactive oxygen species scavenging in Populus. New Phytol. 2024;242(5):2043–58.
58. Chen Y, Li A, Yun P, Chen Q, Pan D, Guo R, Zhang H, Ahmed HAI, Hu H, Peng Y. Genome-wide analysis of MYB transcription factor family and *AsMYB1R* subfamily contribution to ROS homeostasis regulation in *Avena sativa* under PEG-induced drought stress. BMC Plant Biol. 2024;24(1):632.
59. Jiang H-W, Liu M-J, Chen I-C, Huang C-H, Chao L-Y, Hsieh H-L. A glutathione S-transferase regulated by light and hormones participates in the modulation of *Arabidopsis* seedling development. Plant Physiol. 2010;154(4):1646–58.
60. Mano J, Kanameda S, Kuramitsu R, Matsuura N, Yamauchi Y. Detoxification of reactive carbonyl species by glutathione transferase tau isozymes. Front Plant Sci. 2019;10:487.
61. Annunziata MG, Ciarmiello LF, Woodrow P, Dell'Aversana E, Carillo P. Spatial and temporal profile of glycine betaine accumulation in plants under abiotic stresses. Front Plant Sci. 2019;10:230.
62. Stavridou E, Voulgari G, Michailidis M, Kostas S, Chronopoulou EG, Labrou NE, Madesis P, Nianiou-Obeidat I. Overexpression of a biotic stress-inducible *Pvgstu* gene activates early protective responses in tobacco under combined heat and drought. Intern J Mol Sci. 2021;22(5):2352.
63. Li J, Meng L, Ren S, Jia C, Liu R, Jiang H, Chen J. *OsGSTU17*, a tau class glutathione S-transferase gene, positively regulates drought stress tolerance in *Oryza sativa*. Plants. 2023;12(17):3166.
64. Di Toppi LS, Gabbrielli R. Response to cadmium in higher plants. Environ Experiment Bot. 1999;41(2):105–30.
65. Yang Y, Li J, Li H, Ding Y, Wu W, Qin R, Ni J, Xu R, Wei P, Yang J. *OsGSTU5* and *OsGSTU37* encoding glutathione reductases are required for cadmium tolerance in rice. Intern J Environ Sci Technol. 2023;20(9):10253–60.
66. Yu X, Yang L, Fan C, Hu J, Zheng Y, Wang Z, Liu Y, Xiao X, Yang L, Lei T. Abscisic acid (ABA) alleviates cadmium toxicity by enhancing the adsorption of cadmium to root cell walls and inducing antioxidant defense system of *Cosmos bipinnatus*. Ecotoxicol Environ Safety. 2023;261: 115101.
67. Guo R, Li S, Gao YQ, He JT, Wang HY, Chen J, Huang J, Shen RF, Zhu XF. A novel *OsGST* gene encoding 9glutathione reductase negatively regulates cadmium accumulation in rice. J Hazard Mat. 2024;476: 135126.

68. Jing X-Q, Zhou M-R, Nie X-M, Zhang L, Shi P-T, Shalmani A, Miao H, Li W-Q, Liu W-T, Chen K-M. *OsGSTU6* contributes to cadmium stress tolerance in rice by involving in intracellular ROS homeostasis. J Plant Growth Regulat. 2021;40:945–61.
69. Zhang H, Yang J, Li W, Chen Y, Lu H, Zhao S, Li D, Wei M, Li C. *PuHSFA4a* enhances tolerance to excess zinc by regulating reactive oxygen species production and root development in *Populus*. Plant Physiol. 2019;180(4):2254–71.
70. Chen C, Wu Y, Li J, Wang X, Zeng Z, Xu J, Liu Y, Feng J, Chen H, He Y. TBtools-II: A "one for all, all for one" bioinformatics platform for biological big-data mining. Mol Plant. 2023;16(11):1733–42.
71. Wei L, Zhu Y, Liu R, Zhang A, Zhu M, Xu W, Lin A, Lu K, Li J. Genome wide identification and comparative analysis of glutathione transferases (GST) family genes in *Brassica napus*. Scient Rep. 2019;9(1):9196.
72. Li W, Godzik A. Cd-hit. A fast program for clustering and comparing large sets of protein or nucleotide sequences. Bioinformatics. 2006;22(13):1658–9.
73. Gasteiger E, Hoogland C, Gattiker A, Duvaud S, Wilkins MR, Appel RD, Bairoch A. Protein Identification and Analysis Tools on the Expasy Server. In Walker JM, ed. The Proteomics Protocols Handbook. Humana Press; 2005:571-607.
74. Dixon DP, Lapthorn A, Edwards R. Plant glutathione transferases. Genome Biol. 2002;3:1–10.
75. Hasan MS, Singh V, Islam S, Islam MS, Ahsan R, Kaundal A, Islam T, Ghosh A. Genome-wide identification and expression profiling of glutathione S-transferase family under multiple abiotic and biotic stresses in *Medicago truncatula* L. PLoS ONE. 2021;16(2): e0247170.
76. Gong W, Ju Z, Chai J, Zhou X, Lin D, Su W, Zhao G. Physiological and transcription analyses reveal the regulatory mechanism in oat (*Avena sativa*) seedlings with different drought resistance under PEG-induced drought stress. Agronomy. 2022;12(5):1005.
77. Livak KJ, Schmittgen TD. Analysis of relative gene expression data using real-time quantitative PCR and the $2^{-\Delta\Delta CT}$ method. Methods. 2001;25(4):402–8.

Publisher's Note